Linking the Modern Distribution of Biogenic Proxies in High Arctic Greenland Shelf Sediments to Sea Ice, Primary Production, and Arctic-Atlantic Inflow

Limoges, Audrey

2018-03

Limoges , A , Ribeiro , S , Weckström , K , Heikkila , M , Zamelczyk , K , Andersen , T J , Tallberg , P , Masse , G , Rysgaard , S , Norgaard-Pedersen , N & Seidenkrantz , M-S 2018 , ' Linking the Modern Distribution of Biogenic Proxies in High Arctic Greenland Shelf Sediments to Sea Ice, Primary Production, and Arctic-Atlantic Inflow ' , Journal of Geophysical Research : Biogeosciences , vol. 123 , no. 3 , pp. 760-786 . https://doi.org/10.1002/2017JG003840

http://hdl.handle.net/10138/234814
https://doi.org/10.1002/2017JG003840

AGU PUBLICATIONS

JGR

Journal of Geophysical Research: Biogeosciences

RESEARCH ARTICLE
10.1002/2017JG003840

Key Points:
- A new multiproxy reference baseline is provided for assessing past changes in High Arctic fjord and shelf environments
- Cysts of the ice-dwelling dinoflagellate *Polarella glacialis* are tightly connected with seasonal sea ice and show promise as new paleo sea-ice proxy
- Benthic diatoms and ice algae are the main primary producers in the shallower sites, whereas heterotrophic dinoflagellates and benthic foraminifera are indicative of Atlantic water intrusion and dominate at the deeper sites

Supporting Information:
- Supporting Information S1
- Table S1
- Table S2
- Table S3
- Table S4

Correspondence to:
A. Limoges,
audrey.limoges@unb.ca

Citation:
Limoges, A., Ribeiro, S., Weckström, K., Heikkilä, M., Zamelczyk, K., Andersen, T. J., … Seidenkrantz, M-S. (2018). Linking the modern distribution of biogenic proxies in High Arctic Greenland shelf sediments to sea ice, primary production, and Arctic-Atlantic inflow. *Journal of Geophysical Research: Biogeosciences*, *123*, 760–786. https://doi.org/10.1002/2017JG003840

Received 15 MAR 2017
Accepted 4 JAN 2018
Accepted article online 9 JAN 2018
Published online 2 MAR 2018

Linking the Modern Distribution of Biogenic Proxies in High Arctic Greenland Shelf Sediments to Sea Ice, Primary Production, and Arctic-Atlantic Inflow

Audrey Limoges[1,2], Sofia Ribeiro[1], Kaarina Weckström[1,3], Maija Heikkilä[1,3], Katarzyna Zamelczyk[4], Thorbjørn J. Andersen[5], Petra Tallberg[3], Guillaume Massé[6], Søren Rysgaard[7,8], Niels Nørgaard-Pedersen[9], and Marit-Solveig Seidenkrantz[7,10]

[1]Department of Glaciology and Climate, Geological Survey of Denmark and Greenland, Copenhagen, Denmark, [2]Now at Department of Earth Sciences, University of New Brunswick, Fredericton, New Brunswick, Canada, [3]Department of Environmental Sciences, Environmental Change Research Unit, University of Helsinki, Helsinki, Finland, [4]Centre for Arctic Gas Hydrate, Environment and Climate, Department of Geosciences, Arctic University of Norway, Tromsø, Norway, [5]CENPERM, Department of Geosciences and Natural Resource Management, Copenhagen University, Copenhagen, Denmark, [6]UMI3376 TAKUVIK, Department of Biology, CNRS and Université Laval, Quebec City, Quebec, Canada, [7]Arctic Research Centre, Aarhus University, Aarhus, Denmark, [8]Centre for Earth Observation Science, Department of Environment and Geography, University of Manitoba, Winnipeg, Manitoba, Canada, [9]Department of Marine Geology, Geological Survey of Denmark and Greenland, Copenhagen, Denmark, [10]Centre for Past Climate Studies, Department of Geoscience, Aarhus University, Aarhus, Denmark

Abstract The eastern north coast of Greenland is considered to be highly sensitive to the ongoing Arctic warming, but there is a general lack of data on modern conditions and in particular on the modern distribution of climate and environmental proxies to provide a baseline and context for studies on past variability. Here we present a detailed investigation of 11 biogenic proxies preserved in surface sediments from the remote High Arctic Wandel Sea shelf, the entrance to the Independence, Hagen, and Danmark fjords. The composition of organic matter (organic carbon, C:N ratios, $\delta^{13}C$, $\delta^{15}N$, biogenic silica, and IP_{25}) and microfossil assemblages revealed an overall low primary production dominated by benthic diatoms, especially at the shallow sites. While the benthic and planktic foraminiferal assemblages underline the intrusion of chilled Atlantic waters into the deeper parts of the study area, the distribution of organic-walled dinoflagellate cysts is controlled by the local bathymetry and sea ice conditions. The distribution of the dinoflagellate cyst *Polarella glacialis* matches that of seasonal sea ice and the specific biomarker IP_{25}, highlighting the potential of this species for paleo sea ice studies. The information inferred from our multiproxy study has important implications for the interpretation of the biogenic-proxy signal preserved in sediments from circum-Arctic fjords and shelf regions and can serve as a baseline for future studies. This is the first study of its kind in this area.

1. Introduction

As the Arctic warms, the thickness, duration, and extent of the sea ice cover are declining, with significant impacts on both small- and large-scale primary production patterns (Arrigo & van Dijken, 2015; Arrigo et al., 2008; Bélanger et al., 2013; Gradinger, 1995; Kahru et al., 2011; Pabi et al., 2008; Tremblay et al., 2015). Sea ice and snow restrict light transmittance essential for photosynthesis, influence the onset of phytoplankton blooms, and ultimately shape phytoplankton communities. A reduction in the sea ice extent creates more open water habitats for phytoplankton, thus enhancing the length of their growing season. However, regional sea ice loss may alter the convective mixing processes that recycle nutrients into the surface waters during ice formation and naturally trigger algal blooms in spring when the ice breaks up (Niebauer et al., 1990; Stabeno et al., 2010). It is therefore expected that the ongoing warming and associated changes in the sea ice regime will have profound effects on both the abundance and species composition of Arctic algal communities (Arrigo, 2013; Boetius et al., 2013; Loeng et al., 2005; Nöthig et al., 2015; Smetacek & Nicol, 2005; Tremblay et al., 2009), with implications for Arctic ecosystem functioning and biogeochemical cycles.

Another important aspect related to Arctic sea ice melt is the inherent alterations in the freshwater budget at high latitudes (Curry & Mauritzen, 2005; Dickson et al., 2007). Increased export of freshwater and drift ice from the Arctic to the North Atlantic Ocean will impact global ocean circulation and climate through various feedback mechanisms (Aargaard & Carmack, 1989; Clark et al., 2002; Curry et al., 2003; Holland et al., 2007; Jones

et al., 2008; Mauritzen & Hakkinen, 1997; Peterson et al., 2006). Off eastern Greenland, this could translate into strengthened advection of the low salinity Polar surface water carried by the East Greenland Current (EGC) through Fram Strait (Figure 1a) (Dmitrenko et al., 2017; Sejr et al., 2017; Sutherland & Pickart, 2008), the main gateway for Arctic water into the Atlantic Ocean. The sea ice dynamics and local hydrology of Greenlandic fjords and shelf areas further play a critical role for the stability of tidewater outlet glaciers (see Andresen et al., 2012; Bendtsen et al., 2017; Kirillov et al., 2017) and the mass balance of the Greenland ice sheet. Fjord systems located on the eastern North Greenland shelf therefore are key areas for investigating the effects of changing freshwater budgets on the coastal ecosystems.

One way to obtain a retrospective view on the state and change of biological and hydrological parameters in marine settings is to look at the sedimentary remains of various groups of protists (e.g., dinoflagellates, diatoms, and foraminifera). Once settled on the seafloor, the fossil or geochemical remains of the marine protists are incorporated into the sediment, carrying with them the environmental signature of the overlying water masses they inhabited. Diatoms and dinoflagellates constitute two major groups of marine primary producers that thrive in the upper layers of the oceans. Their immediate grazers comprise heterotrophic or mixotrophic dinoflagellates and foraminifera that live at different water-depth intervals within the water column. Accordingly, the fossil remains of diatoms, dinoflagellates, and planktic foraminifera are widely used for investigating past sea surface hydrography, whereas benthic foraminifera are useful proxies for reconstructing subsurface and deep-water mass properties (see Polyak et al., 2010, and references therein). Since they are at the basis of the marine food chain, their assemblage composition and abundances also provide key information on regional paleo-productivity. Unlike the organic-walled cysts of dinoflagellates, which are generally well preserved in the sediment (see, however, Zonneveld et al., 2008), the calcareous (e.g., foraminifera and ostracods) and siliceous (e.g., diatoms and chrysophyte cysts) microfossils can be susceptible to dissolution at high latitudes (e.g., Koç et al., 1993; Matthiessen et al., 2001; Schroeder-Adams & van Rooyen, 2011; Seidenkrantz et al., 2007; Zamelczyk et al., 2012). The absence of siliceous and calcareous fossils from the sediment can therefore be interpreted either as a result of dissolution or low pelagic productivity. A multiproxy approach is thus preferable for making robust inferences of past primary production and hydrographic parameters from high latitudes.

The composition of organic matter in the sediment also provides information on past primary production and specific environmental parameters. The sea ice proxy IP_{25}, a monounsaturated highly branched isoprenoid (HBI) lipid specifically produced by certain sympagic (i.e., ice dwelling) diatom species (Brown et al., 2014), is notably used for reconstructing past trends in Arctic sea ice (Belt et al., 2007; Fahl & Stein, 2012; Hörner et al., 2016; Müller et al., 2009; Stein et al., 2012; Vare et al., 2009, 2010; Xiao et al., 2013). It was recently suggested that studying IP_{25} with its close relative HBI III (triene), likely produced by diatoms blooming in the marginal sea ice zone (Belt et al., 2000), allows for more precise information on past sea ice dynamics (Belt et al., 2015; Smik et al., 2016). However, so far relatively few studies have investigated the use of these proxies in fjord and coastal environments (Brown et al., 2015; Ribeiro et al., 2017).

In this study, we have analyzed a broad suite of biogenic proxies (dinoflagellate cysts, benthic and planktic foraminifera, diatoms, IP_{25}, HBI III, biogenic silica, and elemental and isotopic composition of organic matter) from 16 surface sediment samples collected on the Wandel Sea shelf, the entrance to the Independence fjord, Hagen fjord, and Danmark fjord system (hereafter referred to as Independence fjord system), eastern North Greenland (Figure 1), in relation to present-day sea ice and hydrographic data. Our aim was to establish a reference multiproxy data set that can help in assessing past changes in High Arctic coastal environments, with focus on sea ice conditions and primary production. We also intend to refine the interpretation of the studied proxies through an improved understanding of their distribution in relation to modern conditions. Furthermore, we investigate, for the first time, modern primary producers from the Independence fjord system, one of the most poorly studied fjord systems in Greenland.

2. Materials and Methods

2.1. Regional Settings

The Independence fjord system lies between Peary Land and Kronprins Christian Land in eastern North Greenland (between ~ 80°41′ and 82°27′N; 16°36′ and 32°40′W) (Figure 1b). The fjord system is approximately 150 km long and drains into the Wandel Sea. Two large glaciers, Academy and Hagen, discharge

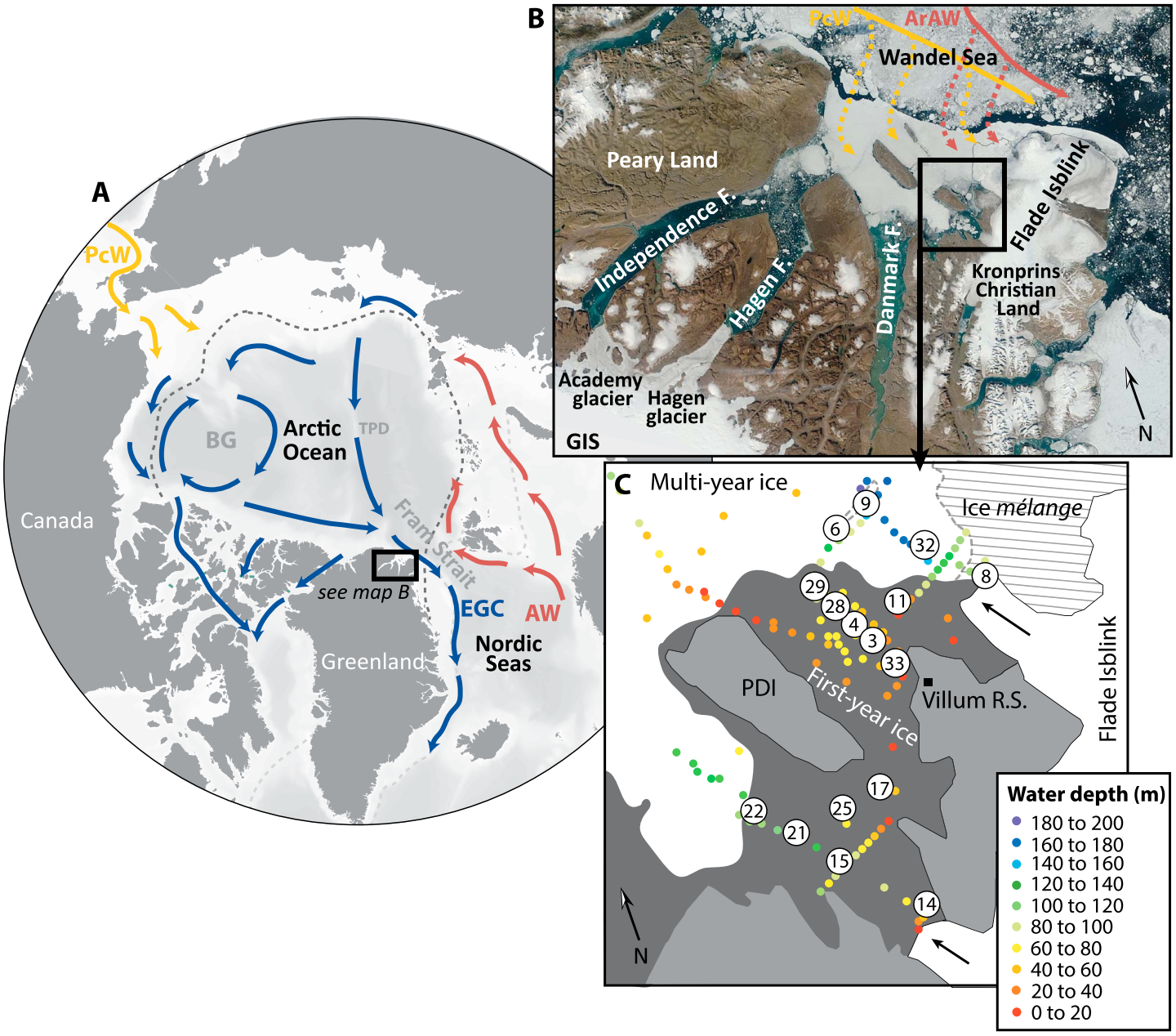

Figure 1. (a) Location of the study area (black rectangle) and schematic illustration of the major circulation patterns in the Arctic Ocean (based on Loeng et al., 2005). The yellow and red arrows indicate the penetration of the North Pacific and Atlantic Waters into the Arctic Ocean. Abbreviations are as follows: PcW, Pacific Waters; AW, Atlantic Waters; TPD, Transpolar Drift; BG, Beaufort Gyre; and EGC, East Greenland Current. The eastern North Greenland region is located directly at the outflow of the Transpolar Drift from the Arctic Ocean, and a major part of the outflows of Arctic Waters occur through Fram Strait, via the East Greenland Current. The dark and light grey dotted lines correspond to the median (1981–2010) extent of the sea ice cover in summer (September) and winter (March), respectively (National Snow and Ice Data Center, nsidc.org/data/seaice_index). (b) Satellite image of the fjord system (image from 13 August 2015; credit: NASA Worldview: https://worldview.earthdata.nasa.gov) and location of the study area (black square). The main regional flows are also illustrated: the Arctic-derived Atlantic water (ArAW) and the Pacific water (PcW) (modified from Kirillov et al., 2017). Abbreviation: GIS, Greenland ice sheet. (c) Bathymetry (m) of the study area (modified from Nørgaard-Pedersen et al., 2016) and location of the surface sediment samples. The region characterized by multiyear sea ice cover is white, whereas the region where sea ice melts seasonally is colored in dark grey (see Figure 2 for annual variability in open water extent for the six years preceding sampling). The striped area corresponds to the region characterized by a *mélange* of sea ice and icebergs. The position of the Villum Research Station (small black square) and Princess Dagmar Island (PDI) is also illustrated. The black arrows represent the Flade Isblink ice cap drainage outlets.

into the head of the Independence and Hagen fjord branches, respectively. The region also supports the largest peripheral ice cap of Greenland, the Flade Isblink ice cap, which covers an area of ~ 7,500 km^2 (Kelly & Lowell, 2009) and drains through two outlets (see Figure 1c) at velocities of a few hundred

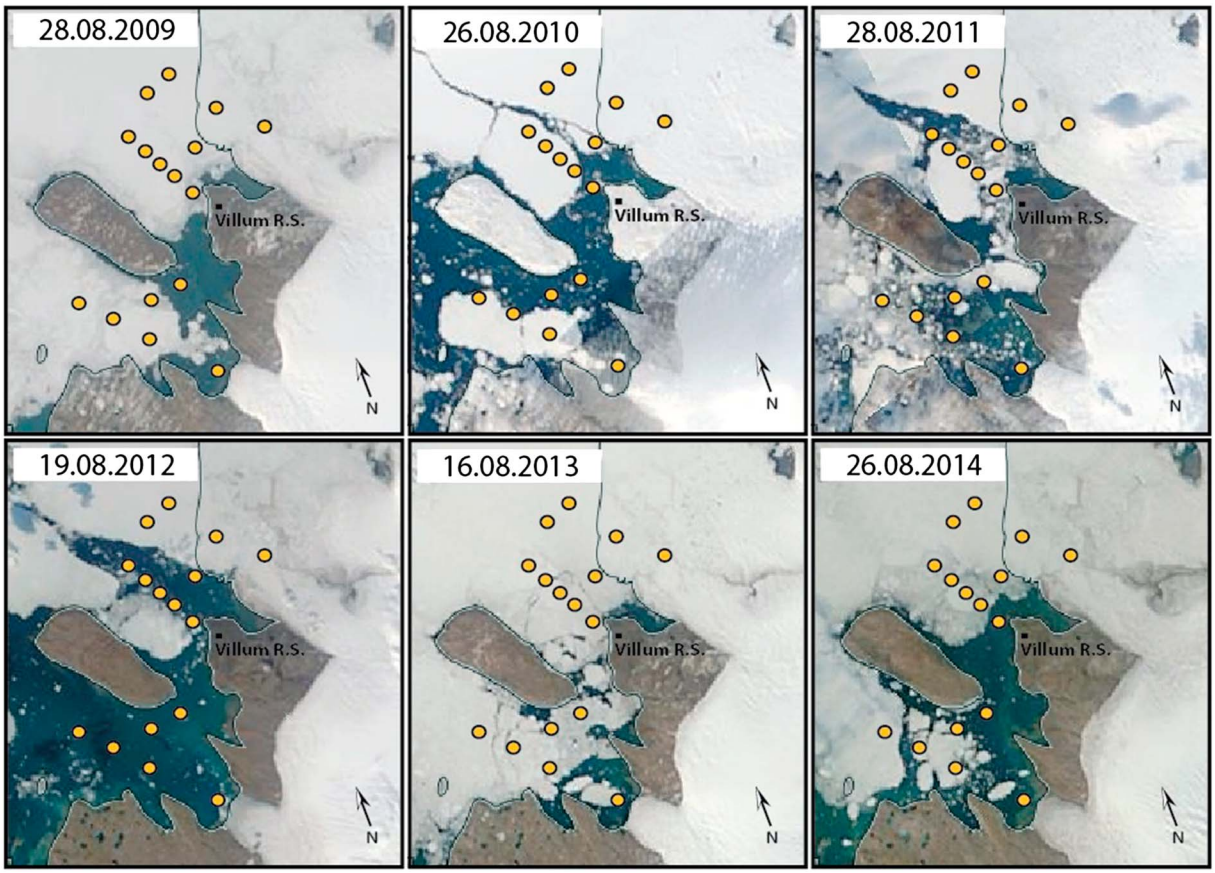

Figure 2. Maximum annual open water extent in the study area based on MODIS imagery (credit: NASA Worldview; https://worldview.earthdata.nasa.gov) for the six years preceding sampling (2009 to 2014). The general outline of the Flade Isblink ice cap front shown in these images is not exactly the same as reported in Figure 1c. Note that we consider the outline presented in Figure 1c to be the most accurate. The sampling sites are illustrated by the yellow circles.

ma^{-1} (Higgins, 1991). Limited information is available for the region, but data from the Danish Meteorological Institute indicate that the fjord system was covered by permanent ice from 1950 to 1964 (Rysgaard et al., 2003). It is only in 1978 that open water leads were first reported in the region through aerial photography (Higgins, 1991).

The geological setting is fairly complex, with Archaic to Paleoproterozoic crystalline basement found closest to the present Greenland ice sheet, unconformably overlain by the proterozoic Independence Fjord Group of alluvial clastic deposits that is cut by dolerites and overridden by proterozoic basalts (Jepsen & Kalsbeek, 1998). Younger siliciclastic and calcareous sedimentary deposits from the late Paleozoic, Mesozoic, and early Cenozoic are found at various, but geographically restricted, locations (Henriksen et al., 2000, 2009). The region was repeatedly glaciated during the Quaternary (Funder, 1989). Following the last deglaciation (Funder, 1989; Nørgaard-Pedersen et al., 2008), the fjord system was inundated by marine waters, and during the Holocene Thermal Maximum (circa 8,000–5,000 years ago) warmer than present summer temperatures may have resulted in open, sea ice-free waters in the summer (Funder et al., 2011).

2.1.1. Present-Day Sea Ice and Hydrographic Conditions

Most of the Independence fjord system is covered by semipermanent sea ice. Only the southern branches of the fjord system and the area adjacent to the Villum Research Station (Station Nord), where the surface sediment samples were collected, are consistently partially ice free during late summer. Satellite images (MODIS) from the area adjacent to the Villum Research Station are available for 6 years preceding sampling (2009 to 2014) (Figure 2). They show that during this time window, sea ice typically started to retreat from the coast at the end of July and formed again in early September—leaving only a little more than a month for open water phytoplankton growth. While there was some variability in the maximum open water extent, the general pattern and timing of sea ice melt and freezeup was relatively consistent over this period.

Table 1
Sampling Site Locations, Water Depth (m), and Sea Ice Thickness as Measured During Fieldwork (Late April 2015)

Sites	Core numbers	Latitude	Longitude	Water depth (m)	Sea ice thickness (m)
1G	k9	81.77878	−16.59632	154.5	1.15
1Fb	k6	81.76615	−16.82502	128	1.25
1O	k32	81.71694	−16.33982	154	3.10
1M	k8	81.67112	−16.02637	111	2.50
1E	k29	81.72030	−17.12090	87	1.30
1D	k28	81.69560	−17.04250	75	1.33
1C	k4	81.67298	−16.96524	73	1.01
1B	k3	81.65198	−16.89640	57	0.99
1K	k11	81.67753	−16.64113	20.8	0.99
1A	k33	81.62295	−16.80726	19.6	0.95
3E	k22	81.53870	−18.05310	115	1.27
3D	k21	81.50400	−17.83700	135	0.99
3F	k25	81.51110	−17.48025	61	1.22
3B	k17	81.51717	−17.21174	54.5	1.22
3C	k15	81.46380	−17.63130	113	1.00
3G	k14	81.39508	−17.21150	55	1.20

The first oceanographic data from the study area are presented in Bendtsen et al. (2017), Dmitrenko et al. (2017), and Kirillov et al. (2017). Conductivity-temperature-depth (CTD) profiles obtained during spring 2015 revealed the origin of the water masses and the interactions with ambient water in the regions deeper than 10 m of our study area. On the Wandel Sea shelf (Figure 1b), the water column can generally be divided into six layers of distinct water masses: a low-salinity surface layer (~1.5–5 m depth) formed by the summer melt of the glaciers and sea ice, a subsurface halocline with a strong vertical salinity gradient down to a depth of 15 m, a Halostad layer of Pacific origin with near freezing temperatures (15–65 m), an Atlantic-modified halocline (65–100 m), Atlantic-modified Polar Water (100–140 m), and relatively warmer and more saline Atlantic bottom waters (>140 m) (Dmitrenko et al., 2017). Accordingly, the deepest sites located North of Princess Dagmar Island (Sites k9–k6; Figure 1c) are the most affected by halocline disturbance caused by Atlantic water intrusions, whereas the hydrological conditions south of Princess Dagmar Island (Sites k22, k21, and k15) seem to be mainly governed by the fjord's ambient waters, and no intrusion of outer-shelf waters was observed in this region. The local influence of cold and turbid subglacial meltwaters originating from the Flade Isblink ice cap was also observed directly at the outlet of the glacier. It has been suggested that subglacial meltwater discharges from marine-terminating glaciers could help promote primary productivity through increased nutrient supplies (e.g., Meire et al., 2017). According to the data from Dmitrenko et al. (2017), the influence of the meltwater originating from this glacier only reaches a few kilometers away from the glacial tongue, only directly affecting Site k8 of this study. No CTD data are available for the southern glacier outlet, near our sampling station k14.

2.2. Methods

Surface sediment samples were collected from the area adjacent to the Villum Research Station (~ 20–30 km from the station) in spring 2015 (Nørgaard-Pedersen et al., 2016). Sampling was conducted while the study area was covered by ice and could be used as a platform for coring. Sediment samples from a total of 16 locations were retrieved using a Van Veen Grab sampler and a Kajak Corer, along transects of varying depths and sea ice thicknesses, starting near the front of the Flade Isblink glacier outlets and the Villum Research station (Figure 1c and Table 1). The sampling sites were targeted based on georeferenced high-resolution radar satellite images, which were used to distinguish between areas of first and multiyear sea ice cover (see Nørgaard-Pedersen et al., 2016). The sediment sampling and coring devices were deployed through holes made in the sea ice with an ice auger, after snow removal. The topmost sediments (0–1 cm) were directly subsampled from the grabs and Kajak cores, subsequently stored at 2–4°C at the Villum Research Station, and transported cooled to Copenhagen. Samples were frozen at −20°C and freeze dried before all analyses were conducted. While sediment mass accumulation rates are not known for all sites, ^{210}Pb and ^{137}Cs analyses were carried out for selected cores (k6, k9, k22, see supporting information). The results show a rapid downcore decline in the activity of unsupported ^{210}Pb, which was generally absent below a depth of 4–6 cm. This suggest sedimentation rates of the order of 4–6 cm/100 years, which must be regarded as

maximum sedimentation rates since a tendency for covariation of the content of unsupported ^{210}Pb and ^{137}Cs indicates that some sediment mixing takes place at the sites.

2.2.1. Grain Size Analysis

The surface sediment was ultrasonically dispersed (2 min on a Bandelin UW 2200) in a sodium pyrophosphate solution and subsequently wet sieved at 1 mm. Particle size analysis was conducted using a Malvern Mastersizer E/2000. The grain size distribution of the samples is reported as percentages of clay, silt, and sand.

2.2.2. Carbon and Nitrogen Elemental and Isotopic Analyses

The freeze-dried surface sediment samples for total organic carbon (TOC) and total nitrogen (TN) analyses were rinsed with distilled water in order to remove the salt residue. For the TOC analysis, samples were treated with hydrochloric acid (HCl, 10%) for 24 h in order to eliminate the inorganic carbon fraction. These samples were then washed with deionized water until the pH of the supernatant equaled that of the deionized water. The sediment for the TOC analyses was freeze dried again. Samples for TOC and nitrogen concentration analyses were weighed (9–150 mg) in tin cups. Elemental analysis was carried out using a MICRO CUBE Elemental Vario elemental analyzer (Laboratory of Geochemistry, University of Helsinki). Lake sediment material (LKSD-4) was used as a reference material. An uncertainty of ±0.1% on the measurements is estimated from replicate analyses of the samples.

Samples for the isotopic composition of bulk organic carbon (δ^{13}C) and nitrogen (δ^{15}N) were rinsed with deionized water. Prior to δ^{13}C analyses, sediment samples were treated with HCl (10%) to eliminate the carbonate fraction. Samples were weighed into tin cups and analyzed with a ThermoQuest Finnigan DeltaPlus XL Isotope Ratio Mass Spectrometer. Replicate measurements of both the samples and a sediment standard "High Organic Content Standard" indicate reproducibility of ±0.5‰ and ±0.2‰ for the sediment material, for δ^{13}C and δ^{15}N respectively. The isotopic ratios are expressed in the δ notation as deviations per mil (‰), so that $\delta_{\text{sample}} = 1000 \times [R_{\text{sample}}/R_{\text{standard}} - 1]$, where R is the ratio of heavy to light isotope (^{13}C/^{12}C or ^{15}N/^{14}N). δ^{13}C values were calibrated to the Vienna Peedee belemnite scale by using the international reference standards USGS41, IAEA-CH3, and IAEA-CH7. δ^{15}N values are expressed relative to atmospheric nitrogen gas, using the international reference standards USGS01, IAEA-N1, and IAEA-N2.

2.2.3. Biogenic Silica

Biogenic silica measurements were conducted at the University of Helsinki following the wet alkaline extraction technique (e.g., DeMaster, 1981). Known weights of sediment samples (30 ± 2 mg) were added to polyethylene bottles and leached for 5 h in a 85°C water bath using 40 mL 1% sodium carbonate (Na_2CO_3). After 3, 4, and 5 h, an aliquot of 1 mL was taken from each sample and analyzed for dissolved silica through spectrophotometry (Perkin Elmer Lambda 25 UV/VIS spectrometer) according to the blue ammonium-molybdate method (Mullin & Riley, 1955). Biogenic silica concentrations were calculated using a linear regression. While mineral-derived silica dissolves at a constant rate throughout the extraction, all biogenic silica is assumed to have dissolved after the first 3 h of the extraction (see, e.g., Barão et al., 2015 for further details).

2.2.4. Biomarkers (Highly Branched Isoprenoids)

Samples for highly branched isoprenoid (HBI) analyses were prepared at Laval University, Quebec, following the procedure described by Belt et al. (2007). An internal standard (7-hexylnonadecane) was added to ~ 0.5 g of freeze dried and homogenized sediment before analytical treatment. Total lipids were ultrasonically extracted (times 3) using a mixture of dichloromethane (DCM: CH_2Cl_2) and methanol (MeOH) (2:1, *v/v*). Extracts were pooled together, and the solvent was removed by evaporation under a slow stream of nitrogen. The total extract was subsequently resuspended in hexane and purified through an open column chromatograph (SiO_2). Hydrocarbons (including IP_{25} and triene (HBI III)) were eluted using hexane (8 mL). Procedural blanks and standard sediments were analyzed every 15 samples.

Hydrocarbon fractions were analyzed using an Agilent 7890 gas chromatograph (GC) fitted with 30 m fused silica Agilent J&C GC columns (0.25 mm i.d. and 0.25 μm phase thickness) and coupled to an Agilent 5975C Series mass selective detector. Oven temperatures were programmed as follows: 40–300°C at 10°C/min, followed by an isothermal interval at 300°C for 10 min. The data were collected using ChemStation and analyzed using MassHunter quantification software. IP_{25} was identified on the basis of retention time and comparison of mass spectra with authenticated standards. Abundances were obtained by comparison of individual GC-mass spectrometry responses against those of the internal standard. For both IP_{25} and HBI III, data are reported in ng g^{-1} sediment.

2.2.5. Diatoms

Diatom analyses were conducted on ~ 0.2 g of freeze-dried sediment that was prepared following standard methodologies (Battarbee et al., 2001). Sediment was oxidized at 90°C for 6 h using hydrogen peroxide (H_2O_2, 30%) in order to remove organic material. Carbonates were then dissolved by addition of a few drops of HCl (35%). The test tubes in which samples were treated were subsequently filled with distilled water and left to settle for 12 h. Residues were then washed several times using demineralized water. A known number of microscopic markers (microspheres) were added to each sample for concentration determinations. A few drops of the final suspension were then dried on a coverslip and subsequently mounted in Naphrax® for light microscopy observation. Identification and quantification were performed using an optical microscope (Leica DMLB), equipped with phase contrast, at a magnification of 1000X. Owing to the generally very low diatom concentrations, the relative abundances of individual taxa are based on counts completed over 10 transects per slide (amounting to ~ 580 microspheres on average).

2.2.6. Dinoflagellate Cysts (Dinocysts) and Other Organic-Walled Microfossils

Samples for palynological analyses were prepared at Ghent University, Belgium, following the standard preparation method described in Quaijtaal et al. (2014). A known weight of freeze-dried sediment (~2–5 g) was rehydrated with demineralized water. A calibrated tablet of *Lycopodium clavatum* spores was added to each sample before treatment in order to estimate the absolute dinocyst concentrations (Stockmarr, 1971). The sediment was repeatedly treated with room-temperature hydrochloric acid (HCl, 2 N) and room-temperature hydrofluoric acid (HF, 40%) to remove calcium carbonate and silicate, respectively. Samples were rinsed stepwise with deionized water. The residues were sonicated for 30 s to break up clusters of amorphous organic matter and sieved through a 10 μm nylon mesh to remove the finer particles. The final residues were mixed with glycerin jelly and mounted on microscope slides. The identification of dinocysts and other organic-walled microfossils was carried out using a light microscope at magnifications of 400X and 1000X. In general, a minimum of two slides was counted per sample, but because of very low cyst concentrations, the total number of counted specimens remains below 300 in every sample. Cysts with visible cell contents were noted.

2.2.7. Foraminifera and Ostracods

For quantitative assemblage analyses, known weights (~1–2 g) of untreated (wet) surface sediment were soaked in tap water, gently sieved through a 63 μm mesh, and subsequently dried. Calcareous benthic and planktic foraminifera from the >63 μm fraction were counted dry on a square-picking tray and identified to the species level. Agglutinated species were not distinguished, but their counts are included in the sums. With the exception of five sites, at least 300 specimens were counted per sample. Ostracod valves were also counted from the same samples, although these were not identified to species level.

3. Results

3.1. Particle Size Analysis

The surface sediment samples were mainly composed of silt (46–81%), with lower proportions of sand (1–38%) and clay (12–35%). Overall, the samples were relatively similar in terms of their grain size distribution. However, the surface sediments from Sites k11, k21, k25, and k28 had sand contents above 25% (Table 2; supporting information).

3.2. Carbon and Nitrogen Elemental and Isotopic Analyses

The total organic carbon (TOC) contents ranged between 0.40 and 2.37 wt % (Figure 3a and Table 2), and total nitrogen (TN) ranged between 0.09 and 0.18 wt % (Table 2). The C:N ratios, which correspond to the ratio between TOC (wt %) and TN (wt %), varied between 3.33 and 15.86 (Figure 3c and Table 2). The highest values were found at Sites k33, k25, k14, and k8 (≥10). The $\delta^{13}C$ values ranged from −26.0 to −23.5‰ ± 0.5‰ (average = −24.9‰) (Figure 3c and Table 2). The sedimentary organic matter from sites north of Princess Dagmar Island was more enriched in ^{13}C compared to the region south of Princess Dagmar Island. The $\delta^{15}N$ values ranged from 2.6 to 5.8‰ ± 0.2‰ (average = 4.8‰) (Figure 3b and Table 2).

3.3. Biogenic Silica

Biogenic silica in sediments is a widely used indicator of paleoproductivity (primarily of diatoms and also radiolarians, silicoflagellates, plant phytoliths, and sponge spicules). Biogenic Silica (BSi) concentrations varied

Table 2
Grain Size Distribution of the Surface Sediment Samples and Contributions to the Sediment of Total Carbon (TC), Nitrogen (TN), and Organic Carbon (TOC) (wt %), Organic Carbon Over Nitrogen Ratios and Carbon and Nitrogen Isotopic Signatures ($\delta^{13}C$, $\delta^{15}N$) of the Sediment (‰)

Core numbers	Clay (%)	Silt (%)	Sand (%)	TC (wt %)	TN (wt %)	TOC (wt %)	C:N	$\delta^{13}C$ (‰)	$\delta^{15}N$ (‰)
k9	15.1	63.9	21.0	1.43	0.14	0.83	5.93	−23.9	5.5
k6	23.4	70.4	6.2	1.31	0.14	0.74	5.29	−26.0	5.8
k32	21.5	72.5	6.0	1.27	0.12	0.67	5.58	−23.7	5.6
k8	34.7	61.7	3.6	2.14	0.17	1.70	10.00	−26.0	4.4
k29	21.4	66.1	12.5	1.20	0.13	0.75	5.77	−23.8	5.6
k28	18.2	56.2	25.6	1.35	0.14	0.69	4.93	−24.4	5.4
k4	24.1	66.4	9.5	1.13	0.12	0.71	5.92	−23.8	5.1
k3	15.7	69.7	14.5	1.33	0.13	0.79	6.08	−24.7	5.3
k11	12.3	59.7	28.0	2.08	0.18	0.92	5.11	−23.7	5.3
k33	15.0	69.7	15.3	1.90	0.18	2.37	13.17	−23.5	5.0
k22	28.6	65.1	6.3	1.26	<DI	0.59	<DI	−25.7	<DI
k21	16.9	45.5	37.6	1.25	0.12	0.40	3.33	−25.8	4.9
k25	14.0	49.1	37.0	2.83	0.14	2.22	15.86	−25.6	2.6
k17	13.5	71.2	15.3	2.00	0.14	1.11	7.93	−25.6	4.1
k15	24.6	71.0	4.4	1.18	0.12	0.69	5.75	−26.0	4.0
k14	17.6	81.0	1.4	2.21	0.09	1.20	13.33	−25.4	2.8

between 0.45 and 4.96 mg g^{-1} dry mass Si (average 1.89 mg g^{-1}) (Figure 4a and Table 3), corresponding to 0.17 to 1.06 wt % SiO_2 (average 0.40 wt % SiO_2). These values are low in comparison with measurements from other high-Arctic fjord regions such as the Young Sound-Tyrolerfjord, where the average value is almost 3 times higher (Ribeiro et al., 2017). This can likely be explained by a longer lasting sea ice cover in the study area, with less biogenic silica accumulating on the seafloor as the result of reduced marine productivity.

3.4. Biomarkers (Highly Branched Isoprenoids)

The biomarker IP_{25} was identified from all sites at low concentrations (from 3.47 to 69.93 ng g^{-1} dry sediment) and is also shown normalized to TOC (μg IP_{25}/g TOC) (Figures 4b and 4c and Table 3). The highest TOC-normalized IP_{25} concentrations were found at the shallow sites with seasonal sea ice cover located in the vicinity of the Villum Research Station (k33 and k11). The lowest concentrations occurred at Sites k9, k6, and sites located south of Princess Dagmar Island (k14, k15, k21, k22, and k25). Triene (HBI III) concentrations were extremely low and ranged from 0 to 0.74 ng g^{-1} dry sediment (Table 3).

3.5. Diatoms

A total of 39 diatom taxa were identified from the sediment samples. The majority of these were benthic species, most of them belonging to the genera *Diploneis*, *Navicula*, and *Nitzschia* (Plate 1). Resting spores of *Chaetoceros* (and one *Thalassiosira antarctica* var. *borealis* spore) were the only planktic taxa found in the samples. Overall abundances were very low, and for Sites k4, k9, k14, k15, and k29 no diatoms were encountered along the analyzed transects (Figure 4d, Table 3, and supporting information). Consistent with high biogenic silica content for the shallow area next to the Villum Research Station, considerably higher diatom concentrations were found at Sites k33 and k11, yielding total counts of ~ 100 valves, whereas only a few valves were found at all other sites. These were also the sites where the majority of species were encountered. Assemblages were dominated by the cosmopolitan marine species *Diploneis nitescens*. Other taxa included the brackish-marine *Diploneis smithii* and *Navicula* cf. *perminuta*; the marine widespread *Fallacia litoricola*, *Nitzschia* cf. *distans*, *Nitzschia* cf. *marginulata*, and *Nitzschia* cf. *rorida*; and the marine (sub)arctic *Pinnularia quadratarea* var. *maxima*. Worth noting is the presence of only two sympagic taxa throughout the study area—*Diploneis litoralis* var. *clathrata* and *Stauroneis* cf. *radissonii*—at very low abundances (<1%). Resting spores of *Chaetoceros* were included in the sums. The good preservation of the diatom valves indicates the absence of significant diatom dissolution, implying that the low diatom abundance at most sites is not a dissolution artifact.

3.6. Dinocysts and Other Organic-Walled Microfossils

Dinocyst concentrations were relatively low with values ranging from 52 to 717 cysts g^{-1} dry sediment (Figure 4e and Table 4). While the highest concentrations were found north of Princess Dagmar Island,

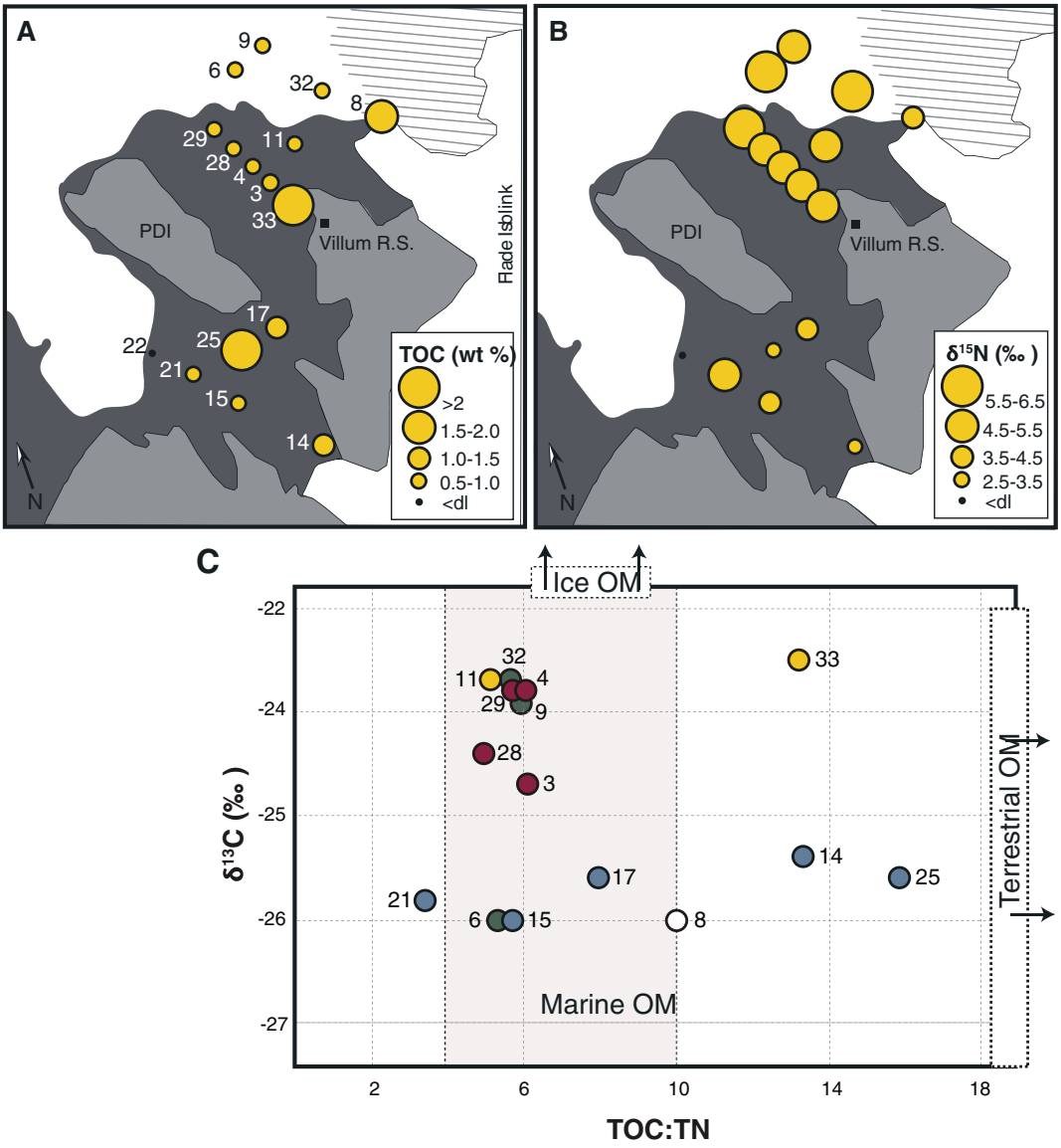

Figure 3. Results from carbon and nitrogen elemental and isotopic analyses. (a) Distribution of total organic carbon (wt %), (b) $\delta^{15}N$ signature of surface sediment (‰), (c) $\delta^{13}C$ values versus TOC:TN ratios of bulk organic matter. The circles indicate the sampling sites. The color code for the sampling sites refers to the subdomains described in section 4.2 (I = blue, II = green, III = red, and IV = yellow). The white boxes represent end-members for ice particulate OM and land-derived OM. The arrows indicate that ice particulate OM is more enriched in ^{13}C compared to pelagic particulate OM values, and land-derived OM yields higher C:N ratio (20 to 100; Meyers, 1994) than aquatic OM. The grey box shows the potential range of values associated to pelagic particulate OM on account of high pCO_2 in cold surface water. Our data indicate varying mixing ratios of pelagic, sympagic, and terrestrial organic carbon in the surface sediment from the fjord system. Higher C:N ratios suggest larger terrestrial input at Sites k25, k14, k33, and k8, whereas enriched $\delta^{13}C$ values may be indicative of higher ice algal input to the sediment.

sites located south of the island and close to the glacier outlets contained only a few cysts, providing very low counts. Nine dinocyst taxa were identified from the surface samples, with seven of them significantly contributing to the assemblages: *Brigantedinium* spp. (mainly *B. simplex*) (6–54%), *Islandinium minutum* (2–47%), *Echinidinium karaense* (0–14%), unspecified "spiny brown cysts" (0–10%), *Polarella glacialis* (0–82%), cf. *Biecheleria* sp. (2–47%), and a cyst here referred to as "round brown type A" (0–4%) (Figure 5a, Plate 2, and supporting information). The spiny brown cyst category encompasses all specimens that could either belong to the genus *Islandinium* or *Echinidinium*, but for which preservation, folding, or orientation did not allow for unequivocal identification. Indeterminate cyst types of probable dinoflagellate affinity were also observed. Although they were not included in the total cyst counts, these taxa are shown in Plate 2.

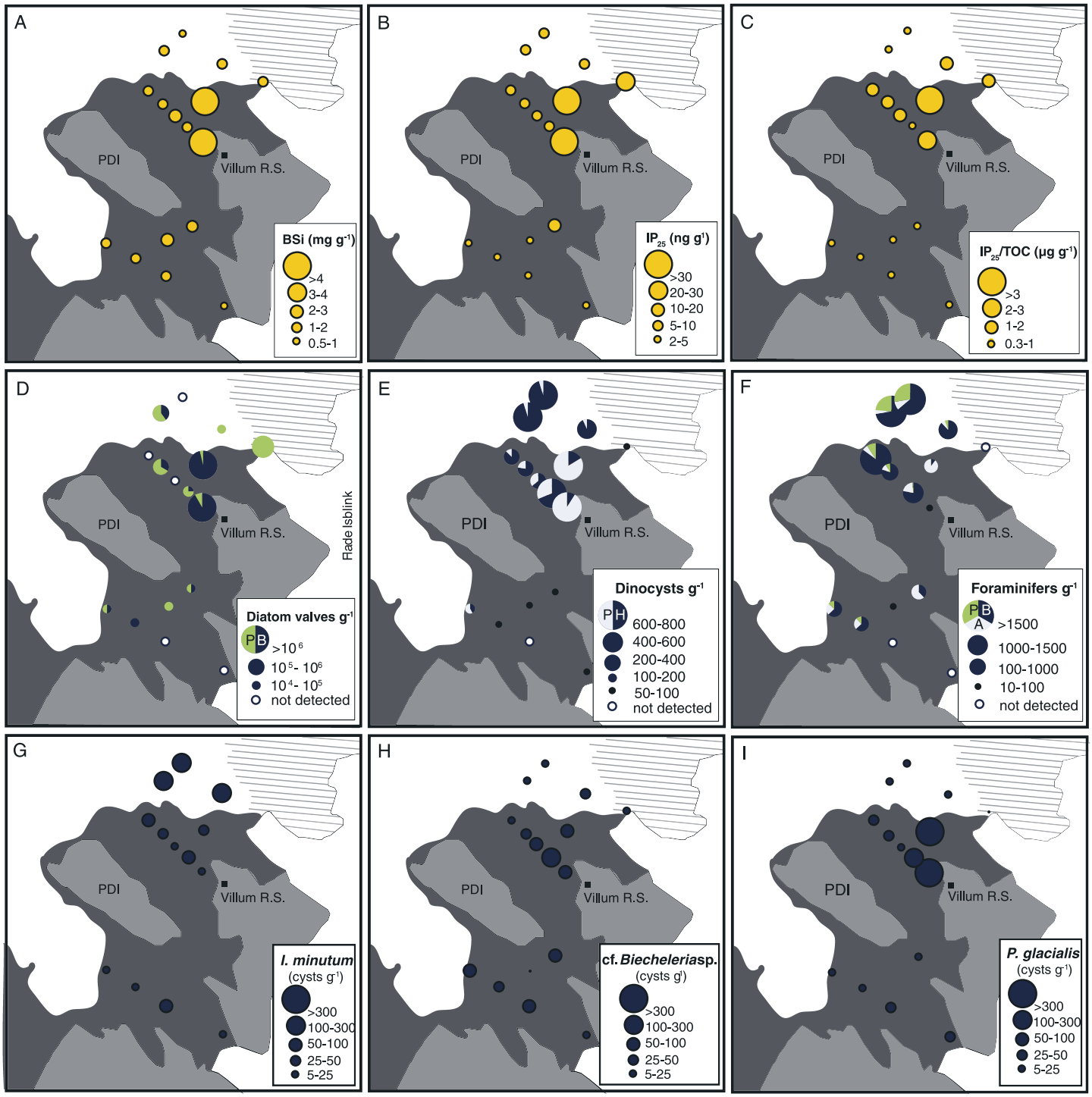

Figure 4. Distribution and concentrations of the main biogenic proxies studied from the surface sediment: (a) biogenic silica (mg g^{-1}); (b) IP_{25} (ng g^{-1}); (c) TOC-normalized IP_{25} (µg g^{-1}); (d) concentrations of diatoms (valves g^{-1}), and proportion of benthic (dark blue) and planktic species, including resting spores of *Chaetoceros* (green); (e) concentrations of dinocysts (cysts g^{-1}) and proportions of phototrophic (light blue) over heterotrophic species (dark blue); (f) concentrations of foraminifera (tests g^{-1}) and proportions of planktic (green), calcareous benthic (dark blue), and agglutinated benthic (light blue) species; (g) concentrations of the heterotroph dinocyst species *Islandinium minutum* (cysts g^{-1}); (h) concentrations of the dinocyst cf. *Biecheleria* sp. (cysts g^{-1}); and (i) concentrations of the phototrophic sea ice dweller dinocyst *Polarella glacialis* (cysts g^{-1}).

Table 3
Biogenic Silica (BSi) (mg g^{-1}), IP_{25} (ng g^{-1}), HBI III (ng g^{-1}), and Total Diatom Concentrations (valves g^{-1})

Core numbers	Bsi (mg g^{-1})	IP_{25} (ng g^{-1})	HBI III (ng g^{-1})	Total diatom concentrations (valves g^{-1})
k9	0.79	7.64	0.04	< 3.91E + 04
k6	1.51	5.79	0.00	2.96E + 05
k32	1.21	7.02	0.11	2.52E + 04
k8	1.15	20.21	0.74	3.89E + 05
k29	1.29	11.38	0.06	< 5.89E + 04
k28	1.17	7.27	0.06	1.04E + 05
k4	2.57	10.79	0.07	< 2.64E + 04
k3	1.71	7.61	0.05	9.70E + 04
k11	4.96	38.49	0.17	1.41E + 06
k33	4.92	69.93	0.23	2.85E + 06
k22	1.73	4.26	0.03	5.09E + 04
k21	1.23	3.47	0.01	6.06E + 04
k25	1.15	3.84	0.15	8.70E + 04
k17	2.87	11.03	0.20	8.85E + 04
k15	1.64	5.03	0.04	< 9.70E + 04
k14	0.45	3.73	0.11	< 7.99E + 04

Foraminiferal linings were very abundant at the deepest Sites (k9 and k6) and at Sites k4 and k3, where they reached concentrations of ~ 20,000 linings g^{-1} (Table 4). The samples also showed a significant presence of the acritarch *Radiosperma corbiferum* and several types of ciliate cysts (Plate 3). While a few reworked cysts were found on most slides, they were particularly abundant at Site k14, which is located directly next to an outlet of the Flade Isblink ice cap (Table 4). Most of these reworked cysts were identified to originate from the Ordovician period, consistent with the bedrock in the fjord catchment, which would indicate input from land rather than in situ reworking of the fjord sediments. Otherwise, a high proportion of the analyzed dinocysts featured visible cellular material, suggesting generally good preservation and/or recent cyst production (see Plate 2).

Important heterogeneities in the spatial distribution and the relative abundances of the dominant species of palynomorphs were recorded. Generally, a fivefold decrease in cyst abundances was observed from the outer to the innermost part of the study area, south of Princess Dagmar Island. This is concomitant with an increase in the proportions of *R. corbiferum* and in the ciliate cysts in the latter region (Figure 5b). With the exception of Site k22, samples from the inner part of the study area yielded very low cyst counts and species' relative abundances were therefore not used for further interpretations.

Classical cluster analysis using a paired-group clustering algorithm and a Euclidean similarity index was carried on the assemblage data for samples with total cyst counts higher than 60. The resulting dendrogram clearly highlights the important compositional shift in the assemblages for the region north of Princess Dagmar Island (Figure 5a). Sites located at shallow depths (k11 and k33), close to the Villum Research Station, are the most dissimilar of all sites. These sites are characterized by a striking dominance of the phototrophic species *P. glacialis*. It is also at these sites that the highest total cyst concentrations were recorded. On the contrary, heterotrophic species belonging to *Brigantedinium* spp. and spiny brown sensu lato (e.g., *I. minutum*, *Islandinium*? *cezare*, *E. karaense*, and other unspecified spiny brown) were prevalent at the deepest sites (k6, k9, and k32), where the sea ice cover is semipermanent. Intermediate cyst abundances and diversity were found to characterize sites located between these two compositional poles (k29, k28, k3, and k4), where assemblages are still mainly composed of heterotrophic species. Finally, although Site k22 features a bathymetry and general sea ice conditions close to that of the deepest sites located north of Princess Dagmar Island, this sample forms its own group possibly owing to the significant proportion of phototrophic species (mainly cf. *Biecheleria* sp.).

3.7. Foraminifera and Ostracods

Concentrations of total foraminifera varied from 0 to 2,714 tests g^{-1} (Table 4). Whereas calcareous and agglutinated benthic foraminifera were present at most studied sites, planktic species were only present in significant abundances (>800 tests g^{-1}) at the deepest sites (k6 and k9) (see Figure 4). In total, 37 species of calcareous benthic and 3 species of planktic foraminifera were identified (Table 5). The main benthic species included *Cassidulina neoteretis* (7 to 53%), *Cassidulina reniforme* (0 to 32%), *Elphidium hallandense* (0–63%), *Elphidium clavatum* (often described as *E. excavatum* f. *clavata*) (0–46%), *Epistominella arctica* (0–30%), *Stetsonia horvathi* (0–22%), *Cibicides lobatulus* (0–18%), *Buccella frigida* (0–12%), *Elphidium albiumbilicatum* (0–9%), *Triloculina trihedra* (0–11%), *Quinqueloculina* sp. (0–10%), *Stainforthia loeblichi* (0–7%), and *Islandiella helenae* (0–6%) (Figure 6, Plate 4, and supporting information). The planktic foraminiferal assemblages are dominated by *Neogloboquadrina pachyderma* sinistral (0–97%) and *Turborotalita quinqueloba* (0–26%), accompanied by lower abundances of *Neogloboquadrina incompta* (0–14%) (Figure 6). Note that all right coiling *N. pachyderma* in all samples with more than 3% of right coiling *N. pachyderma* are identified as *N. incompta* (Sites k1, k3, k21, and k32), and in all samples with less than 3% they are called *N. pachyderma* (the rest of the samples) (cf. Darling et al., 2006).

Plate 1. Differential interference contrast photomicrographs of the diatom taxa recovered from the surface samples. 1–2: *Diploneis nitescens*, 3: *Diploneis smithii* var., 4: *Navicula* sp.1, 5: *Fallacia litoricola*, 6: *Navicula* sp.2, 7: *Trachyneis aspera*, 8: *Navicula cf. wunsamiae*, 9–10: Nitzschia cf. *rorida*, 11: *Nitzschia* cf. *marginulata* var. Scale bars represent 10 μm.

In the study area, a calcareous fauna prevails at the deepest sites, where total abundances also are at their highest (Figure 4). In contrast, assemblages from the shallowest sites are mostly composed of agglutinated species and yielded very low total concentrations. Owing to the relatively shallow environmental setting

Table 4
Total Concentrations of Modern Dinocysts (cysts g^{-1}), Reworked Dinocysts (cysts g^{-1}), Organic Linings of Foraminifera (linings g^{-1}), and *Foraminifera, Including Benthic and Planktic Species (tests g^{-1})*

Core numbers	Modern dinocysts (cysts g^{-1})	Reworked dinocysts (cysts g^{-1})	Organic linings of foraminifera (linings g^{-1})	Foraminifera (tests g^{-1})
k9	717	9	16136	2714
k6	705	34	17580	1871
k32	492	82	7539	1063
k8	85	43	503	<Dl
k29	363	77	4727	1570
k28	359	17	8943	838
k4	231	61	20890	n/a
k3	709	233	13666	1011
k11	783	42	629	164
k33	659	62	923	75
k22	129	0	3867	887
k21	85	13	3226	388
k25	52	26	619	23
k17	76	0	991	129
k15	93	5	2351	<dl
k14	58	498	16	<dl

(20 to 160 m), the low abundance and diversity of planktic foraminifera at most sites is not surprising. Their marked presence (719 individual g^{-1}) at the deepest sites is however noteworthy.

Ostracods were common in four samples (k6, k9, k29, and k33) and absent to rare in the other samples. Abundances ranged from 0 to 45 individuals g^{-1}.

4. Discussion

4.1. Source of Organic Matter

The organic matter C:N ratios and $\delta^{13}C$ can be used to discriminate between terrestrial versus marine sources of organic matter (OM) deposited in the sediments. Phytoplankton and zooplankton have atomic C:N ratios ranging between 4 and 10, whereas these are generally above 20 for terrestrial vascular plants (Meyers, 1994). The $\delta^{13}C$ signature indicates both the dynamics of carbon assimilation during photosynthesis and isotopic composition of the carbon source (Hayes, 1993; Meyers, 1997). In general, aquatic OM (between −22 and −20‰) is more enriched in ^{13}C than terrestrial OM (~ −27‰) (Belicka & Harvey, 2009; Meyers, 1994; Naidu et al., 2000). The carbon isotopic signature is, however, more complicated in Arctic environments where high pCO_2 and slow algal growth in cold surface water can lead to depleted $\delta^{13}C$ values approaching those of terrestrial OM (Pineault et al., 2013; Rau et al., 1989), while enriched ice algal OM (2–10‰ more enriched than pelagic OM; Hobson & Welch, 1992; Søreide et al., 2006) has an opposite influence on the values. Enriched $\delta^{13}C$ values associated to ice algal OM are due to limited atmospheric CO_2-exchange under sea ice, which eventually results in reduced ^{13}C discrimination during photosynthesis as biomass increases and the pool of dissolved inorganic carbon declines (Fischer, 1991; Kerby & Raven, 1985; Rau et al., 1992). Thus, the range of marine $\delta^{13}C$ values in the Arctic is broad (−34.7 to −18‰) (Goericke & Fry, 1994; Pineault et al., 2013). For example, particulate OM in Northeast Water Polynya, off northeastern Greenland, has $\delta^{13}C$ values between −28 and −27‰ (Hobson et al., 1995) and ice algae around −18.5‰. These $\delta^{13}C$ values are comparable to those reported from the Arctic Ocean (Schubert & Calvert, 2001), where pelagic and ice particulate OM $\delta^{13}C$ values range between −24.2 to −27.6‰ and −18.3 to −20.6‰, respectively.

Carbon isotope values at our stations indicate a mixed input of marine and terrestrial sources. More enriched values (higher than −24‰ $\delta^{13}C$) are recorded in the relatively higher productivity region north of the Villum Research Station, while more depleted values are recorded south of Princess Dagmar Island (around −26‰). The OM from terrestrial sources is more clearly distinguished by higher C:N values at stations k25, k14, k33, and k8 (Figure 3). The more enriched $\delta^{13}C$ at k33 compared to other stations with high C:N values could be due to high ice algal input as indicated by high concentrations of *P. glacialis* and IP_{25} (Figure 4). It is also important to note that our C:N ratios were not corrected to remove potential land-derived inorganic nitrogen (ammonium attached to clay minerals), which can lead to underestimated C:N values in Arctic clay-rich sediments (see Kumar et al., 2016). This could affect Site k8 in particular, where the clay content is 34.7%, although this clay content is low in comparison to other Arctic sediments (Stein et al., 1994).

4.2. Environmental Interpretation

The reliability of environmental reconstructions from biogenic proxies strongly relies on existing information about the different species-specific ecological requirements (temperature, salinity, sea ice cover, nutrient and food availability, sediment substrate, etc.), and the chemical properties of their fossil remain. In the study area, we found no evidence for poor preservation of the fossil assemblages. Because the foraminiferal linings counted from palynological slides are likely the remnants of benthic calcareous species (Jennings et al., 2014), a comparison between these and the tests found in the sediment can indicate the degree of carbonate dissolution (De Vernal et al., 1992). At most stations, the relatively similar trends in both records indicate good preservation of calcareous material (R^2 = 0.75; see supporting information). The differences in their

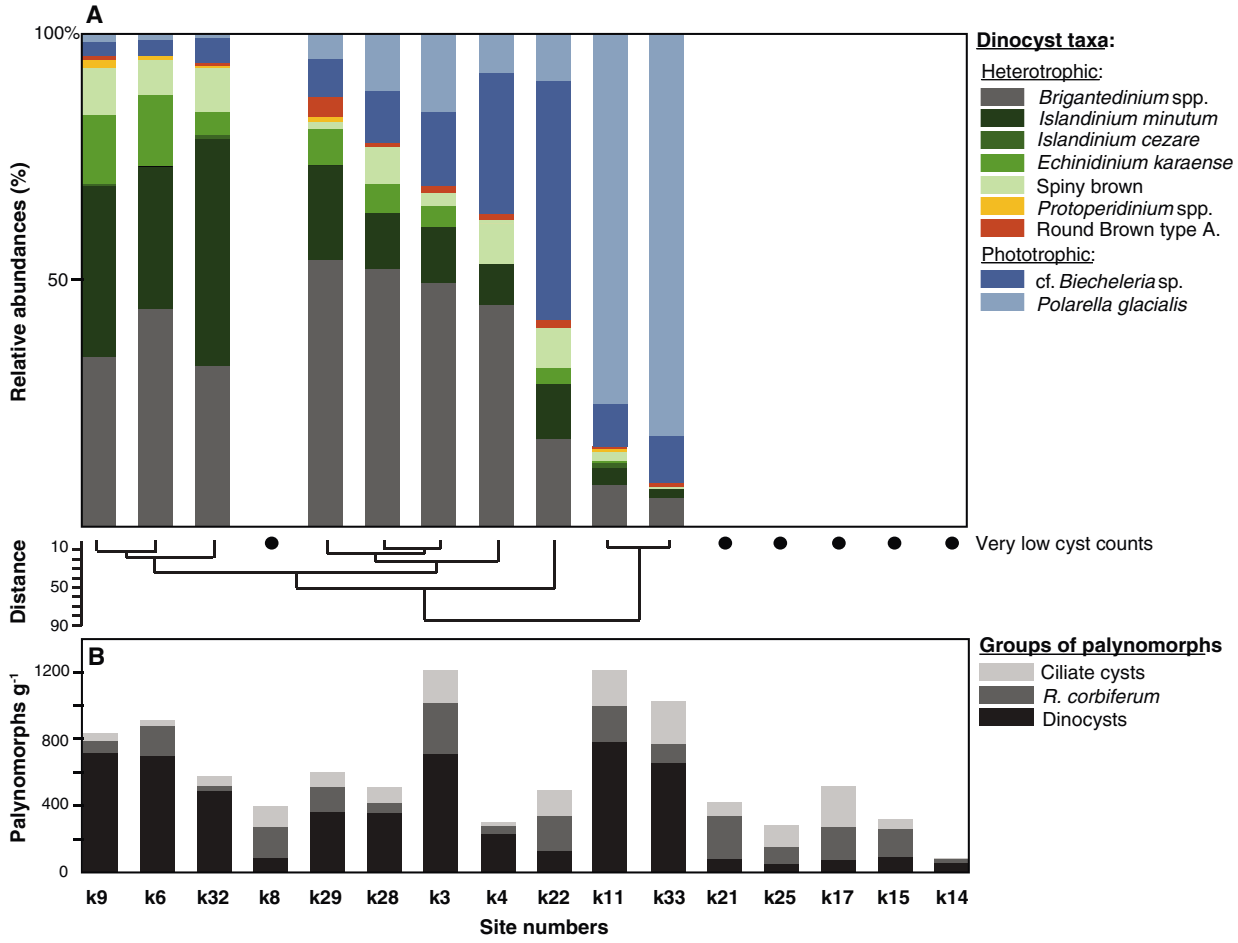

Figure 5. (a) Dinocyst assemblage composition diagram and dendrogram resulting from the cluster analysis. The dots indicate sites with very low cyst counts (<30 cysts), which were not included in the cluster analysis. (b) Total abundance of three groups of palynomorphs (g^{-1} of dry sediment). Dinocysts are shown in black, the acritarch *Radiosperma corbiferum* in dark grey, and the ciliate cysts in light grey. Note the low contribution of dinocysts to the total palynomorph abundances from station k21 onward in parallel with a slight increase in the contribution of *R. corbiferum*.

abundances are likely the result of the different sizes of the analyzed fractions; linings were studied from the palynological residues in the fraction between 10 and 106 μm, while tests were counted in the hand-sieved bulk sediment, from the fraction larger than 63 μm.

Similarly, the generally good state of preservation of the diatom valves does not suggest that the assemblages were affected by dissolution. Consequently, it is assumed that changes in the composition of the fossil assemblages reflect the ecological conditions influencing the living assemblages. Accordingly, the spatial structure in the proxy data fairly closely follows the interplay between the bathymetry, water masses, and sea ice conditions, and four assemblage subdomains were defined:

1. *Subdomain I*: *Region south of Princess Dagmar Island (Sites k14, k15, k17, k21, k22, and k25)*. Surface sediments from this region contained low concentrations of marine microfossils and biomarkers. Furthermore, depleted $\delta^{15}N$ values can be indicative of low nitrate utilization, assuming that the nitrate pool is not limited (Altabet & Francois, 1994). Within the main groups of organic-walled microfossils, *R. corbiferum* dominates over dinocysts, which are almost absent. The biological affinity of *R. corbiferum* is currently unknown, but this acritarch is commonly reported from brackish environments or inner-shelf settings with low surface salinities (Kunz-Pirrung, 1999; Matthiessen et al., 2000; Milzer et al., 2013; Sorrel et al., 2006). The assemblages likely indicate lower salinities in this area. Although hydrographical measurements are very scarce for this subdomain, the area does not appear to be influenced by offshore-advected water masses (Dmitrenko et al., 2017). Similar to what has been observed in other

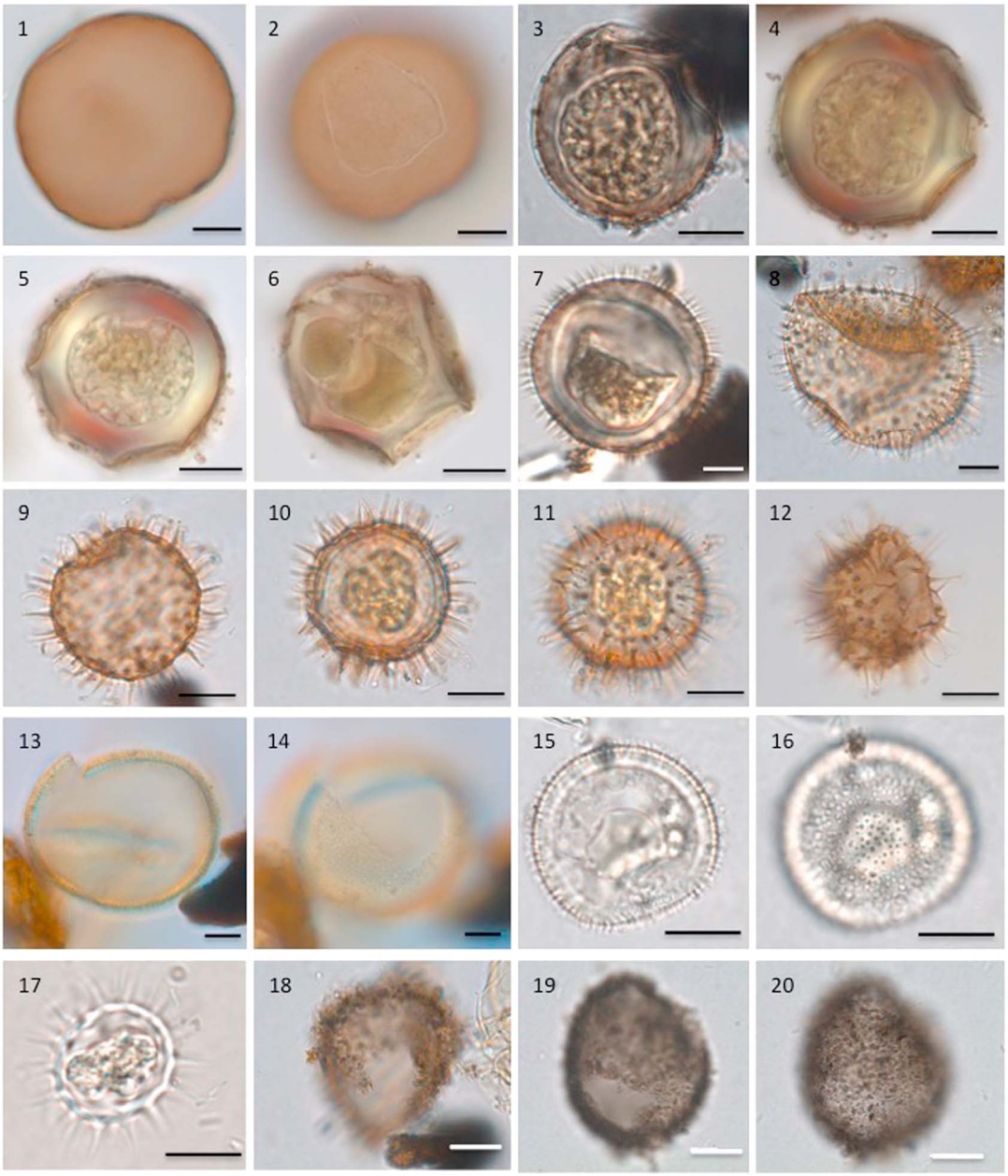

Plate 2. Bright-field photomicrographs of the main dinocyst taxa recovered from the surface samples. 1–2: high and low focal views of the same specimen of *B. simplex*, 3–6: midfocal views of different specimens of the round brown type A., 7–8: midfocal views of two different specimens of *I. minutum*, 9: midfocal view of *E. karaense*, 10–11: midfocal and high focal views of the same specimen of *E. karaense,* 12: midfocal view of *E. karaense*, 13–14: midfocal and low focal views of *B. tepikiense*, 15–16: midfocal and high focal views of cf. *Biecheleria* sp., 17: midfocal view of *P. glacialis*, 18: high view of the indeterminate cyst type, 19–20: high focal and midfocal views of the same specimen of the indeterminate cyst type. Scale bars represent 10 μm.

High Arctic settings (cf. Mueller et al., 2003), the bathymetry and sea ice dynamics south of Princess Dagmar Island possibly create a physically constrained basin that allows pooling of freshwater derived from the southern branch of the fjord drainage basin (Kirillov et al., 2017). This seems consistent with the very low salinity (16–21) recorded from the water layer directly below the ice during the oceanographic campaign of 2015 (Dmitrenko et al., 2017).

2. *Subdomain II: Outermost and deeper sites (Sites k9, k6, and k32)*. This subdomain comprises sites from the deepest part of our study area, under the influence of a semipermanent sea ice cover. The nitrogen isotopic signature is the most enriched ($\delta^{15}N$ between 5.5 and 5.8‰), which could reflect high nitrate utilization in sea ice relative to the water column (Fripiat et al., 2014). However, in oligotrophic Arctic

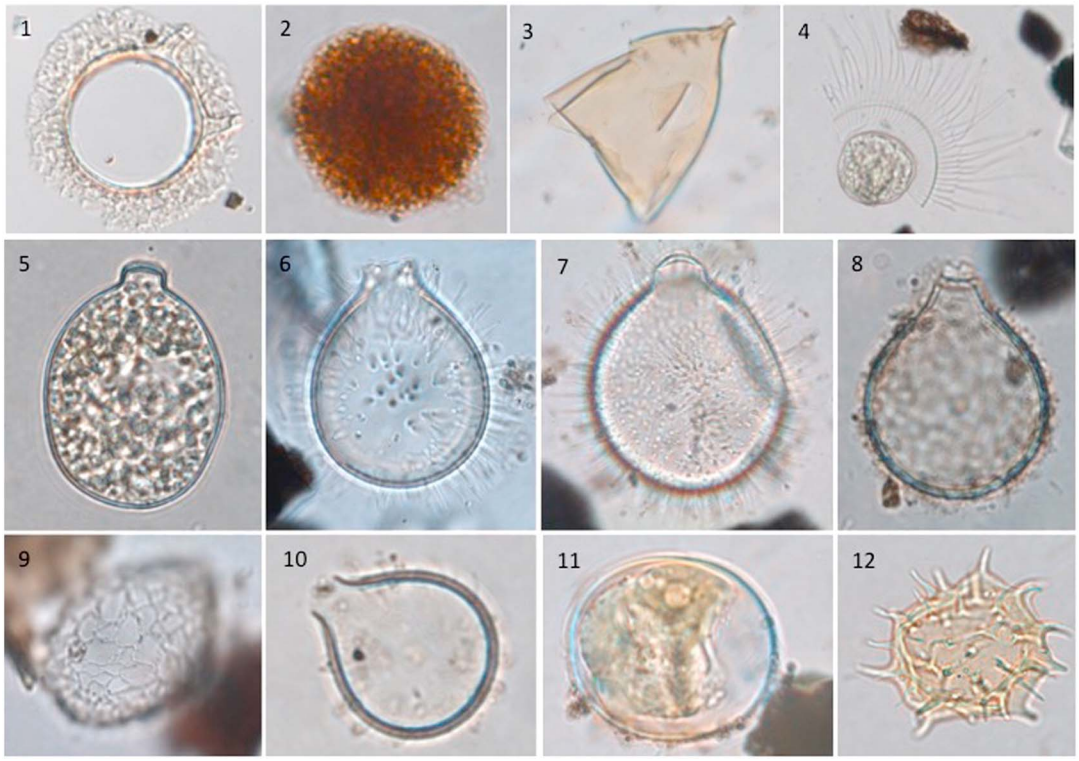

Plate 3. Bright-field micrographs of organic-walled microfossils recovered from the surface samples. 1: acritarch type A, 2: acritarch type B, 3: Turbellaria oocyte?, 4: *Radiosperma corbiferum*, 5: ciliate cyst type B, 6: ciliate cyst type C, 7: ciliate cyst sp., 8: ciliate cyst sp., 9: ciliate cyst sp., 10: ciliate cyst type A, 11: unidentified medium-sized cell with cell content, and 12: reworked Ordovician acritarch sp.

systems nitrate is typically also limited in the water column, leading to overlapping $\delta^{15}N$ ranges in sympagic and pelagic OM (Kohlbach et al., 2016; Pineault et al., 2013). Phototrophic organisms (diatoms and autotrophic dinoflagellates) are nearly absent; this is consistent with limited light penetration. Surprisingly, however, their potential grazers (heterotrophic dinoflagellates, ciliates, and foraminifera) are present in relatively high abundances. Dinocyst assemblages are dominated by species belonging to the *Protoperidinium/Archaeperidinium* and Diplopsalid groups, notably *Brigantedinium simplex*, *Islandinium minutum*, and *Echinidinium karaense*. These cysts are typically found in sediments from marine settings characterized by prolonged seasonal sea ice cover (de Vernal et al., 2001; Rochon et al., 1999). Their cyst production, however, appears to take place during the open water period (Heikkilä et al., 2016). Similarly, foraminiferal assemblages are diverse and composed of benthic and planktic species, the latter mainly consisting of *N. pachyderma* (sinistral) and *T. quinqueloba*. Although some polar species possibly feed on phytodetritus (Cornelius & Gooday, 2004), *N. pachyderma* is known to feed primarily on diatoms (Hemer et al., 2007; Salvi et al., 2006; Volkmann, 2000) and *T. quinqueloba* is especially abundant in frontal zones and other high-productivity regions (Johannessen et al., 1994; Nørgaard-Pedersen et al., 2007). Considering the sea ice thickness of the order of 1.15–1.25 m for Sites k9 and k6 compared to 3.10 m for Site k32 measured during the field campaign (late April 2015), our data can be interpreted in different ways: (1) The semipermanent sea ice cover restrains in situ primary production, but tests of planktic foraminifera and dinocysts are advected from the productive offshore open waters via subsurface currents. This would explain why the grazers are found in the sediment, while the primary producers are extremely scarce. Following this line of reasoning, however, one might expect more planktic diatom valves since their size and weight make them more prone to lateral transport than the heavy tests of foraminifera (de Vernal et al., 2006). (2) The semipermanent sea ice cover restrains in situ primary production, but food supply is advected from the productive offshore open waters via nutrient-rich subsurface currents. (3) Flaw leads sometimes open in the sea ice, allowing for short-term algal blooms that sustain a relatively broad autochthonous foraminiferal and dinoflagellate community. However, due to efficient grazing, the remains of diatoms and phototrophic

Table 5
List of Dinocyst, Foraminiferal and Diatom Taxa Encountered in the Surface Sediment Samples

Dinocyst taxa		Foraminiferal taxa		Diatom taxa	
Phototrophic taxa	Heterotrophic taxa	Calcareous benthic	Planktic	Benthic	Planktic
Polarella glacialis (Montresor et al., 1999)	*Brigantedinium simplex* (Wall, 1967; ex Lentin & Williams, 1993)	*Buccella frigida* (Cushman, 1921)	*Neogloboquadrina pachyderma* (Ehrenberg, 1861)	*Amphora laevis* (Gregory, 1857)	*Thalassiosira antarctica* var. borealis (Fryxell et al., 1981) spore
cf. *Biecheleria* sp.	*Brigantedinium* (Reid, 1977; ex Lentin & Williams, 1993) spp.	*Cassidulina neoteretis* (Seidenkrantz, 1995)	*Neogloboquadrina incompta* (Cifelli, 1961)	*Amphora proteus* (Gregory, 1857)	*Chaetoceros* (Ehrenberg, 1844) resting spores
Bitectatodinium tepikiense (Wilson, 1973)	*Islandinium minutum* (Harland & Reid in Harland et al. 1980; Head et al. 2001)	*Cassidulina reniforme* (Nørvang, 1945)	*Turborotalita quinqueloba* (Natland, 1938)	*Amphora* spp.	
Operculodinium centrocarpum Arctic morphotype sensu (de Vernal et al., 2001)	*Islandinium? cezare* (de Vernal et al., 1989 ex de Vernal in Rochon et al. 1999; Radi et al., 2013)	*Cassidulina laevigata* (d'Orbigny, 1826)		*Bacillaria paxillifer* (Müller, 1786; Marsson, 1901)	
	Echinidinium karaense (Head et al., 2001; Radi et al., 2013)	*Cibicides lobatulus* (Walker & Jacob, 1798)		*Cocconeis scutellum* (Ehrenberg, 1838)	
		Cibicides wuellerstorfi (Schwager, 1866)		*Cymbella* spp.	
		Cornuspira involvens (Reuss, 1850)		*Diploneis litoralis* var. *clathrata* (Østrup, 1895; Cleve, 1896)	
		Elphidium albiumbilicatum (Weiss, 1954)		*Diploneis nitescens* (Gregory 1857; Cleve 1894)	
		Elphidium bartletti (Cushman, 1933)		*Diploneis smithii* var.	
		Elphidium clavatum (Cushman, 1930)		*Diploneis subcincta* (Schmidt, 1874; Cleve, 1894)	
		Elphidium hallandense (Brotzen, 1943)		*Diploneis* spp.	
		Elphidium sp.		*Fallacia litoricola* (Hustedt, 1955; Mann, 1990)	
		Epistominella arctica (Green, 1959)		*Gyrosigma* cf. *spenceri* (Smith, 1852; Griffith & Henfrey, 1856)	
		Epistominella sp.		*Gyrosigma* spp.	
		Fissurina spp.		*Karayevia clevei* (Grunow, 1880; Round & Bukhtiyarova, 1999)	
		Guttulina dawsoni (Cushman & Ozawa, 1930)		*Navicula directa* (Smith 1853; Ralfs, 1861)	
		Guttulina sp.		*Navicula kariana* var. *frigida* (Grunow 1880; Cleve, 1895)	
		Islandiella helenae (Feyling-Hanssen & Buzas, 1976)		*Navicula* cf. *microdigitoradiata*	
		Islandiella norcrossi (Cushman, 1933)		*Navicula obtusangula* (Hustedt, 1942)	
		Lagena elongata (Dunikowski, 1879)		*Navicula peregrina* (Ehrenberg 1843; Kützing, 1844)	
		Lagena striata (d'Orbigny, 1939)		*Navicula* cf. *perminuta* (Grunow, 1880)	

Journal of Geophysical Research: Biogeosciences 10.1002/2017JG003840

Journal of Geophysical Research: Biogeosciences 10.1002/2017JG003840

Table 5 *(continued)*

Dinocyst taxa		Foraminiferal taxa		Diatom taxa	
Phototrophic taxa	Heterotrophic taxa	Calcareous benthic	Planktic	Benthic	Planktic
		Melonis barleeanus (Williamson, 1958)		*Navicula phyllepta* (Kützing, 1844)	
		Milliolinella sp.		*Navicula* cf. *wunsamiae* (Witkowski et al., 2000)	
		Nonionellina labradorica (Dawson, 1860)		*Navicula* spp.	
		Oolina sp.		*Nitzschia* cf. *arctica*	
		Parafissurina spp.		*Nitzschia* cf. *distans* (Gregory, 1857)	
		Patellina corrugata (Williamson, 1958)		*Nitzschia marginulata* (Grunow, 1880)	
		Pyrgo williamsoni (Silvestri, 1923)		*Nitzschia* cf. *marginulata* var.	
		Pyrgoella irregularris (d'Orbigny, 1839)		*Nitzschia* cf. *rorida* (Giffen, 1975)	
		Quinqueloculina arctica (Cushman, 1933)		*Nitzschia* cf. *sigma* (Kützing, 1844; Smith, 1853)	
		Quinqueloculina sp.		*Nitzschia* spp.	
		Robertinoides sp.		*Pinnularia quadratarea* var. maxima	
		Stainforthia loeblichi (Feyling-Hanssen, 1954)		*Pinnularia quadratarea* var. minor	
		Stainforthia concava (Höglund, 1947)		*Planothidium delicatulum* (Kützing) (Round & Bukhtiyarova, 1996)	
		Stetsonia horvathi (Green, 1959)		*Pleurosigma* spp.	
		Triloculina trihedra (Loeblich & Tappan, 1953)		*Stauroneis* cf. *radissonii* (Poulin & Cardinal, 1982)	
		Triloculina sp.		*Synedra tabulata* (Agardh) (Kützing, 1844)	
				Trachyneis aspera (Ehrenberg) (Cleve, 1894)	

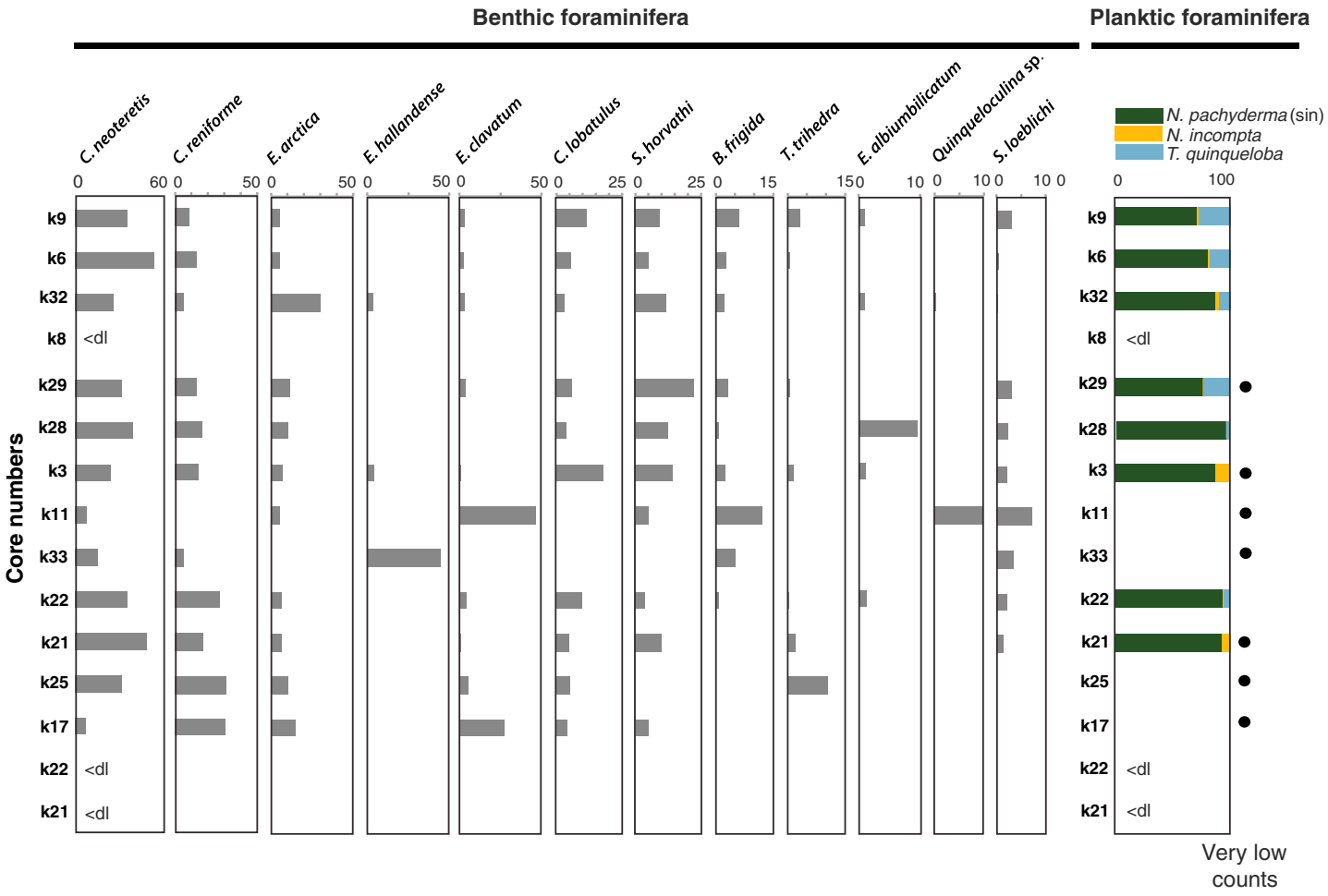

Figure 6. Benthic and planktic foraminiferal percentages in the >63 μm fraction. The dots indicate sites with very low planktic foraminiferal counts (<35 tests). Sites k8, k22, and k21 were virtually barren of foraminifera.

dinocysts do not settle in the sediment. In all cases, the marine signature of the sedimentary assemblages strongly suggests this area is under marine influence.

3. *Subdomain III. Transect of decreasing depths (Sites k29, k28, k4, and k3)*. Although dinocyst abundances are conspicuously lower in this subdomain than in subdomains II and IV, gradual changes in the total abundances of foraminifera as well as in the ratio of heterotrophic/phototrophic dinocysts are observed with decreasing distance to the coast. This transient proxy signature appears to be primarily linked to (1) varying bathymetry that impacts the structure of the water column, and (2) the dynamics of sea ice retreat, which likely affects the timing of light availability for phytoplankton growth.
4. *Subdomain IV. Shallower sites (Sites k11 and k33)*. This shallow area (below 40 m depth) is located in the region of early seasonal sea ice retreat (July ice edge) and corresponds to the local productivity "hot spot". With the exception of the foraminifera, all biogenic proxies display their peak abundances here, clearly illustrating that conditions are most favorable for photosynthetic activity. Furthermore, enriched $\delta^{15}N$ values relative to the region south of Princess Dagmar Island reflect higher nitrate utilization. This is however only under the assumption that diagenetic enrichment (Robinson et al., 2012) of $\delta^{15}N$ affects all the study sites similarly. The bathymetry conditions and dynamics of sea ice retreat further suggest that IP_{25} is locally produced. Together with cf. *Biecheleria* sp., the sea ice dwelling *P. glacialis* dominates the dinocyst assemblages. The latter species is known to produce cysts in sea ice brine in the spring (Stoecker et al., 1997) and has been recorded in sediment traps directly after the ice breakup (Heikkilä et al., 2016). Benthic calcareous foraminifera are only present at low concentrations, and their assemblages are dominated by *E. clavatum* and *E. arctica*. The opportunistic species *E. clavatum* is widespread on the Arctic

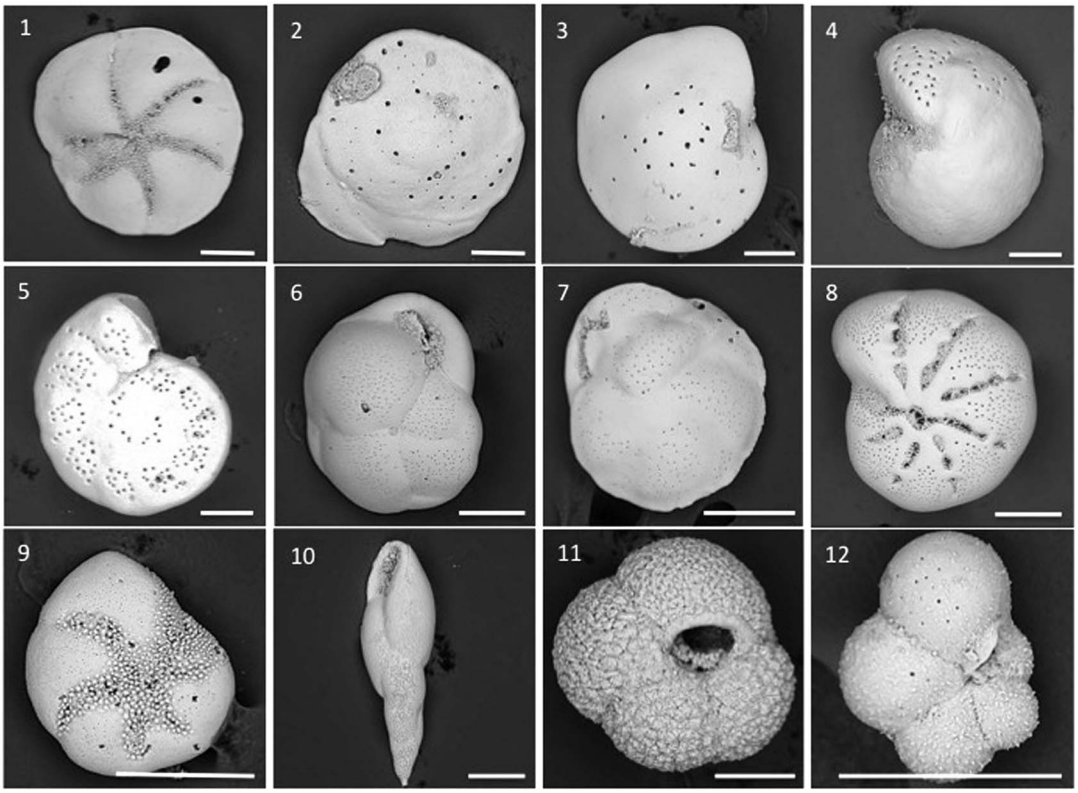

Plate 4. SEM micrographs of the main species of foraminifera recovered from the surface samples. 1–2: *Buccella frigida*, 3: *Islandiella helenae*, 4–5: *Cibicides lobatulus*, 6: *Cassidulina reniforme*, 7: *Cassidulina neoteretis*, 8: *Elphidium clavatum*, 9: *Elphidium albiumbilicatum*, 10: *Stainforthia loeblichi*, 11: *Neogloboquadrina pachyderma* sinistral, and 12: *Turborotalita quinqueloba*. Scale bars: 100 μm.

shelves, including extreme environments such as near tidewater glacier fronts (Hald et al., 1994; Hald & Korsun, 1997; Korsun & Hald, 1998, 2000; Leslie, 1965; Mudie et al., 1983). The exceptional ability of this species to adapt to harsh environments may be related to its high nutritional and habitat versatility, and its capability to quickly colonize seafloor areas that are temporarily suitable for growth (Alve, 1999; Corliss, 1991; Corliss & Van Weering, 1993; Linke & Lutze, 1993; Wollenburg & Mackensen, 1998). Furthermore, *E. arctica* shows an affinity to areas with both low productivity and high seasonal production (Cornelius & Gooday, 2004; Pawlowski, 1991; Wollenburg & Mackensen, 1998); this suggests that this species is capable of adapting to contrasting conditions (Wollenburg & Kuhnt, 2000). All proxies are indicative of typical glacio-marine conditions that are seasonally favorable for algal blooms in this area.

4.3. Primary Production

Photosynthetic organisms at the base of the food web modulate the amount of fresh organic matter available for the upper trophic levels; this plays a key role in ecosystem functioning. In our study area, notable spatial heterogeneity in primary production can be inferred from the various biogenic tracers.

Although the low diatom, dinocyst, TOC, and biogenic silica contents that prevail at most sites suggest overall low primary production—coherent with short periods of photosynthetically favorable light conditions—enhanced production is nonetheless recorded in the subdomain IV (Sites k11 and k33). Despite a clear sedimentary signal from ice-derived algae (e.g., the dinocyst *P. glacialis*), the markedly higher diatom concentrations at these sites dominated by benthic diatoms suggests that the microphytobenthos contributes to a significant fraction of the local primary production. A dominance of benthic over pelagic productivity has been documented from other Arctic fjord regions (Glud et al., 2002, 2009) and was further suggested to predominate in oligotrophic areas (Glud et al., 2009). Sediment-dwelling diatoms have the ability to rapidly adjust to fluctuating light conditions (Kühl et al., 2001, Wulff et al., 2008, 2009; Karsten et al., 2011) and

efficiently use the nutrients released by mineralization processes in the sediment underneath (Glud et al., 2009; Karsten et al., 2011). A number of species have proven to be able to withstand several months of complete darkness (Wulff et al., 2008). In addition to benefiting from extended growth season, benthic diatoms possess a clear advantage over pelagic organisms when nutrients are limited.

Although our multiproxy approach only allows for investigating the response of a selection of primary producers to their environment, diatoms are often considered the most important functional group within the microphytobenthos in marine coastal regions (MacIntyre et al., 1996; Karsten et al., 2011). Whether dynamic interactions take place between the benthic and sea ice habitats for optimal food acquisition cannot be unraveled from our data, but the fact that the concentrations of benthic diatoms exceed those of planktic and sympagic diatoms in subdomain IV clearly indicates that the benthic community fulfills a significant ecological role in this system, as in other High Arctic fjords.

4.4. Sea Ice Conditions

The only known producers of IP_{25} are marine benthic diatoms belonging to *Haslea* (*H. spicula* and *H. kjellmanii*) and *Pleurosigma* (*P. stuxbergii* var. *rhomboides*) (Brown et al., 2014; G. Massé and M. Poulin, personal communication, 2017). These species typically flourish on the underside of sea ice, near the ice-water interface (Brown et al., 2011). In addition to other constraining environmental factors (e.g., salinity and nutrients), their growth strongly depends upon a complex interplay between sea ice occurrence and sufficient light availability. The presence of IP_{25} at all sites suggests the presence of IP_{25}-producing taxa in the ice from the fjord system—although none of the above species were observed from the fossil assemblages (IP_{25}-producing species typically represent ~ 1–5% of Arctic sea ice assemblages (Belt et al., 2013) and their frustules do not preserve in the sediments)—and reflects the regional thinning and melting of the ice cover over the summer months. However, with the exception of Sites k11 and k33, the generally low contents of the biomarker in the sediment suggest that the conditions are probably not optimal for IP_{25}-producing taxa to grow. This is particularly apparent in the region south of Princess Dagmar Island, where sea ice conditions similar to those in the northern region do not lead to comparable sediment IP_{25} concentrations. A change in the dominant groups of palynomorphs in this region as well as the $\delta^{13}C$, $\delta^{15}N$, and C:N signature of the organic matter also points to a lower salinity. This is consistent with observations from Ribeiro et al. (2017), Xiao et al. (2013), and Hörner et al. (2016), where low sedimentary IP_{25} concentrations were linked to reduced salinities. IP_{25} is produced in the ice and released when the sea ice melts, in contrast to HBI III, which is thought to be produced in open waters by diatoms possibly blooming near the marginal ice zone (Belt et al., 2000), although not exclusively (Belt et al., 2017). In our study area, HBI III concentrations are extremely low, supporting a very short period of open water.

Interestingly, the regional patterns of IP_{25} and cysts belonging to the dinoflagellate *P. glacialis* are very similar (R^2 = 0.80; see supporting information), and for both proxies, peak abundances are found at Sites k11 and k33. *P. glacialis* is a very halotolerant sea ice-dwelling dinoflagellate (Montresor et al., 1999; Zheng et al., 2012). This species was first recorded from land-fast sea ice in McMurdo Sound (Antarctica; Stoecker et al., 1997), and it has since been found to have a circumpolar distribution (Montresor et al., 2003). The tiny cysts ($<$20 μm) produced by this photosynthetic dinoflagellate have, however, rarely been reported from marine sediment samples. Only Heikkilä et al. (2014, 2016) and Kunz-Pirrung (1998) have reported *P. glacialis* from sediment samples, from the Hudson Bay and Laptev Sea, respectively. Note that Kunz-Pirrung (1998) identified and illustrated *P. glacialis* cysts as "Acritarch type A". It is difficult to disentangle the possible effects of the poor resistance to degradation in the sediment and/or water column and loss during palynological preparations from its near absence from paleoenvironmental study records (Heikkilä et al., 2016). In the study area *P. glacialis* occurs in all samples, except Sites k25 and k8, where overall cyst abundances are extremely low ($<$90 cysts g^{-1}). Furthermore, the absolute abundance of *P. glacialis* reaches values in the order of 500 cysts g^{-1} at the shallow Sites k11 (20.8 m) and k33 (19.6 m), which represent a critical area in terms of local sea ice retreat. *P. glacialis* is the only dinoflagellate species known today to be able to complete its biological cycle in the sea ice and produces potentially fossilizable resting cysts. Cysts of *P. glacialis* further appear to be well preserved in the Independence Fjord system. We therefore recommend a careful consideration of their presence in sedimentary archives as they have the potential to represent an extremely valuable proxy for tracing past sea ice conditions.

The presence of cf. *Biecheleria* sp. at all studied sites is also noteworthy. These cysts appear to be an important component of the assemblages from High Arctic fjord regions and Hudson Bay (Heikkilä et al., 2016). At present, the ecological preferences of this species and its relation to sea ice cover are poorly known, but its presence is important in the study area, contributing to the diversity of the assemblages.

4.5. Tracing Arctic-Atlantic Inflow

The overall faunal composition and prevalence of benthic foraminifera is typical for East Greenland fjords and shelf margins (Andresen et al., 2013; Jennings & Helgadottir, 1994; Perner et al., 2015). The distribution of the main foraminiferal species further seems to be strongly modulated by the structure of the water column, which is, in turn, partly shaped by the bathymetry of the study area. The highest concentrations of both calcareous benthic and planktic species were found at the deepest sites (k9, k6, k32, and k29), and concentrations dropped considerably with decreasing depth. *C. neoteretis* and *C. reniforme* dominate the assemblages from all sites, except for the shallow Sites k11 and k33. Both species are infaunal and generally inhabit shallow shelf to deep-sea environments (150–3000 m) (Hald & Korsun, 1997; Seidenkrantz, 1995). In modern Greenland and Svalbard shelf and fjord environments, *C. neoteretis* thrives in relatively cool (−1 to 2°C), saline (34.9 practical salinity unit, psu) bottom water conditions, and *C. reniforme* prefers colder water (<2°C) and also relatively high salinity (>30 psu) environments (Hald & Korsun, 1997; Jennings et al., 2004; Polyak, Korsun, et al., 2002; Polyak, Levitan, et al., 2002; Steinsund et al., 1994). Thus, in Arctic shelf regions, both species are commonly associated with the advection of chilled subsurface Atlantic waters (Bartels et al., 2017; Hald & Korsun, 1997; Jennings et al., 2004; Lubinski et al., 2001; Mackensen & Hald, 1988; Polyak & Mikhailov, 1996; Polyak, Levitan, et al., 2002; Seidenkrantz et al., 2013). The relatively high abundance of *N. pachyderma* and the presence of heterotrophic dinocyst species in an area characterized by semiperennial sea ice cover (subdomain II) would further support the advection of Atlantic waters through subsurface currents, as planktic foraminifera likely do not live here and the specimens would all have been carried to the site from the open shelf.

CTD measurements from the outer fjord region (Dmitrenko et al., 2017) show the presence of subsurface freshened waters of Pacific origin (Halostad), which overlie a deeper layer of Atlantic-modified Polar Water. Here an intrusion of relatively saline bottom waters can clearly be inferred from the microfaunal assemblages. Also, since the bottom water masses appear to be associated with relatively high abundances of foraminifera and heterotrophic dinocysts, it is likely that surface conditions supported significant primary productivity. Finally, in line with the observations of Dmitrenko et al. (2017), the area surrounding Site k32 appears to be less influenced by this intrusion. This is underlined by lower foraminiferal and dinocyst total abundances but similar assemblage compositions.

5. Conclusions

Our multiproxy investigation provides a robust foundation for investigating past environmental changes, particularly regarding the interplay of sea ice, primary production, and hydrography along eastern North Greenland, one of the most sensitive regions to the ongoing Arctic warming. Furthermore, this study provides new insights into the distribution of the sea ice species *Polarella glacialis* and its cysts, which have the potential to become a useful proxy for reconstructing past seasonal sea ice. Further work on their preservation potential in sediment archives and during palynological preparation treatments is needed.

A number of important points can also be made.

1. Microfossil preservation is generally good, providing a strong modern baseline for future studies.
2. Overall modern primary production is low, consistent with limited light availability, and is largely governed by the sea ice conditions and bathymetry.
3. The microphytobenthos contributes to a significant fraction of the local primary production, especially in the shallow parts of the fjord.
4. Based on the microfossil and geochemical signal, the study area could be divided into four ecological subdomains linked to bathymetry, water mass distribution, sea ice cover, and primary production.
5. The distribution of benthic foraminifera generally reflects the major bottom water masses and can be used to trace changes in the Arctic inflow in relation with changes in the Arctic sea ice cover.

Acknowledgments
The raw data obtained in this study are available in the supporting information. This study received financial support from the Villum Foundation, Denmark (grant VKR023454 to SRi.). Field work was funded by the Arctic Research Centre, Aarhus University, and the Villum Foundation. The Department of Environmental Science, Aarhus University is acknowledged for providing logistics at Villum Research Station in North Greenland. A. L. was also funded by the Fonds de Recherche du Québec - Nature et technologies (FRQNT grant 188947). M. H. was also funded by the Academy of Finland (grant 296895). SRy was funded by the Canada Excellence Research Chair program (CERC grant 214902). M. S. S. was funded through the Danish Council for Independent Research (DFF-FNU grants 0602-02361B, OceanHeat) and the Independent Research Fund Denmark (grant 7014-00113B, G-Ice). We thank Kunuk Lennert, Jesper Hofmann, and Egon R. Frandsen for technical and logistical assistance in the field. We also appreciate outstanding logistical support from the Station Nord Danish military personnel. We further thank Leonid Polyak and Steffen Aagaard Sørensen for useful advice on benthic foraminiferal identification, Andrzej Witkowski for help with diatom taxonomy, and Laurence Dyke for commenting on the manuscript. This work is a contribution to the Arctic Science Partnership (ASP) and the ArcticNet Networks of Centres of Excellence programs.

References

Aargaard, K., & Carmack, E. C. (1989). The role of sea ice and other fresh water in the Arctic circulation. *Journal of Geophysical Research*, *94*(C10), 14485–14,498. https://doi.org/10.1029/JC094iC10p14485

Altabet, M. A., & Francois, R. (1994). Sedimentary nitrogen isotopic ratio as a recorder for surface ocean nitrate utilization. *Global Biogeochemical Cycles*, *8*(1), 103–116. https://doi.org/10.1029/93GB03396

Alve, E. (1999). Colonization of new habitats by benthic foraminifera: A review. *Earth-Science Reviews*, *46*(1-4), 167–185. https://doi.org/10.1016/S0012-8252(99)00016-1

Andresen, C. S., Hansen, M. J., Seidenkrantz, M.-S., Jennings, A. E., Knudsen, M. F., Nørgaard-Pedersen, N., … Pearce, C. (2013). Mid- to late-Holocene oceanographic variability on the Southeast Greenland shelf. *The Holocene*, *23*(2), 167–178. https://doi.org/10.1177/0959683612460789

Andresen, C. S., Straneo, F., Ribergaard, M. H., Bjørk, A. A., Andersen, T. J., Kuijpers, A., … Ahlstrøm, A. P. (2012). Rapid response of Helheim Glacier in Greenland to climate variability over the past century. *Nature Geoscience*, *5*, 37–41.

Arrigo, K. R. (2013). The changing Arctic Ocean. *Elementa Science of the Anthroprocene*, *1*, 1–5.

Arrigo, K. R., & van Dijken, G. L. (2015). Continued increases in Arctic Ocean primary production. *Progress in Oceanography*, *136*, 60–70. https://doi.org/10.1016/j.pocean.2015.05.002

Arrigo, K. R., van Dijken, G. L., & Pabi, S. (2008). Impact of the shrinking Arctic ice cover on marine primary production. *Geophysical Research Letters*, *35*, L19603. https://doi.org/10.1029/2008GL035028

Barão, L., Vandevenne, F., Clymans, W., Frings, P., Ragueneau, O., Meire, P., … Stuyf, E. (2015). Alkaline-extractable silicon from land to ocean: A challenge for biogenic silicon determination. *Limnology and Oceanography: Methods*, *13*(7), 329–344. https://doi.org/10.1002/lom3.10028

Bartels, M., Titschack, J., Fahl, K., Stein, R., Seidenkrantz, M.-S., Hillaire-Marcel, C., & Hebbeln, D. (2017). Effects of Atlantic Water on northern Spitsbergen's glaciers since 15500 years. *Climate of the Past*, *13*(12), 1717–1749. https://doi.org/10.5194/cp-13-1717-2017

Battarbee, R. W., Jones, V. J., Flower, R. J., Cameron, N. G., Bennion, H., Carvalho, L., & Juggins, S. (2001). Diatoms. In J. P. Smol (Ed.), *Tracking environmental change using lake sediments. Terrestrial, algal, and siliceous indicators* (Vol. 3, pp. 155–202). Dordrecht, Netherlands: Kluwer.

Bélanger, S., Babin, M., & Tremblay, J.-É. (2013). Increasing cloudiness in Arctic damps the increase in phytoplankton primary production due to sea ice receding. *Biogeosciences*, *10*(6), 4087–4101. https://doi.org/10.5194/bg-10-4087-2013

Belicka, L. L., & Harvey, R. H. (2009). The sequestration of terrestrial organic carbon in Arctic Ocean sediments: A comparison of methods and implications for regional carbon budgets. *Geochimica et Cosmochimica Acta*, *73*(20), 6231–6248. https://doi.org/10.1016/j.gca.2009.07.020

Belt, S. T., Allard, G. W., Massé, G., Robert, J.-M., & Rowland, S. J. (2000). Highly branched isoprenoids (HBIs): Identification of the most common and abundant sedimentary isomers. *Geochimica et Cosmochimica Acta*, *64*(22), 3839–3851. https://doi.org/10.1016/S0016-7037(00)00464-6

Belt, S. T., Brown, T. A., Smik, L., Tatarek, A., Wiktor, J., Stowasser, G., … Husum, K. (2017). Identification of C_{25} highly branched isoprenoid (HBI) alkenes in diatoms of the genus Rhizosolenia in polar and sub-polar marine phytoplankton. *Organic Geochemistry*, *110*, 65–72. https://doi.org/10.1016/j.orggeochem.2017.05.007

Belt, S. T., Cabedo-Sanz, P., Smik, L., Navarro-Rodriguez, A., Berben, S. M. P., Knies, J., & Husum, K. (2015). Identification of paleo Arctic winter sea ice limits and the marginal ice zone: Optimized biomarker-based reconstructions of late Quaternary Arctic sea ice. *Earth and Planetary Science Letters*, *431*, 127–139. https://doi.org/10.1016/j.epsl.2015.09.020

Belt, S. T., Massé, G., Rowland, S. J., Poulin, M., Michel, C., & Leblanc, B. (2007). A novel chemical fossil of palaeo sea ice: IP_{25}. *Organic Geochemistry*, *38*(1), 16–27. https://doi.org/10.1016/j.orggeochem.2006.09.013

Belt, S. T., Brown, T. A., Ringrose, A. E., Cabedo-Sanz, P., Mundy, C. J., Gosselin, M., & Poulin, M. (2013). Quantitative measurement of the sea ice diatom biomarker IP25 and sterols in Arctic sea ice and underlying sediments: Further consideration for paleo sea ice reconstructions. *Organic Geochemistry*, *62*, 33–45. https://doi.org/10.1016/j.orggeochem.2013.07.002

Bendtsen, J., Mortensen, J., Lennert, K., Ehn, J. K., Boone, W., Galindo, V., … Rysgaard, S. (2017). Sea ice breakup and marine melt of a retreating tidewater outlet glacier in northeast Greenland (81°N). *Scientific Reports*, *7*(1), 4941. https://doi.org/10.1038/s41598-017-05089-3

Boetius, A., Albrecht, S., Bakker, K., Bienhold, C., Felden, J., Fernández-Méndez, M., … Wenzhöfer, F. (2013). Export of algal biomass from the melting Arctic sea ice. *Science*, *339*(6126), 1430–1432. https://doi.org/10.1126/science.1231346

Brown, T. A., Belt, S., Mundy, C., Philippe, B., Massé, G., & Poulin, M. (2011). Temporal and vertical variations of lipid biomarkers during a bottom ice diatom bloom in the Canadian Beaufort Sea: Further evidence for the use of the IP_{25} biomarker as a proxy for spring Arctic sea ice. *Polar Biology*, *34*(12), 1857–1868. https://doi.org/10.1007/s00300-010-0942-5

Brown, T. A., Belt, S. T., Tatarekm, A., & Mundy, C. J. (2014). Source identification of the Arctic sea ice proxy IP_{25}. *Nature Communications*, *5*, 4197.

Brown, T. A., Hegseth, E. N., & Belt, S. T. (2015). A biomarker-based investigation of the mid-winter ecosystem in Rijpfjorden, Svalbard. *Polar Biology*, *38*(1), 37–50. https://doi.org/10.1007/s00300-013-1352-2

Clark, P. U., Pisias, N. G., Stocker, T. F., & Weaver, A. J. (2002). The role of the thermohaline circulation in abrupt climate change. *Nature*, *415*(6874), 863–869. https://doi.org/10.1038/415863a

Corliss, B. H. (1991). Morphology and microhabitat preferences of benthic foraminifera from the northwest Atlantic Ocean. *Marine Micropaleontology*, *17*(3-4), 195–236. https://doi.org/10.1016/0377-8398(91)90014-W

Corliss, B. H., & Van Weering, T. C. E. (1993). Living (stained) benthic foraminifera within surficial sediments of the Skagerrak. *Marine Geology*, *111*(3-4), 323–335. https://doi.org/10.1016/0025-3227(93)90138-L

Cornelius, N., & Gooday, A. J. (2004). 'Live' (stained) deep-sea benthic foraminifera in the western Weddell Sea: trends in abundance, diversity and taxonomic composition along a depth transect. *Deep-Sea Research Part II*, *51*(14-16), 1571–1602. https://doi.org/10.1016/j.dsr2.2004.06.024

Curry, R., Dickson, B., & Yashayaev, I. (2003). A change in the freshwater balance of the Atlantic Ocean over the past four decades. *Nature*, *426*(6968), 826–829. https://doi.org/10.1038/nature02206

Curry, R., & Mauritzen, C. (2005). Dilution of the northern North Atlantic Ocean in recent decades. *Science*, *308*(5729), 1772–1774. https://doi.org/10.1126/science.1109477

Darling, K. F., Kucera, M., Kroon, D., & Wade, C. M. (2006). A resolution for the coiling direction paradox in *Neogloboquadrina pachyderma*. *Paleoceanography*, *21*, PA2011. https://doi.org/10.1029/2005PA001189

De Vernal, A., Bilodeau, G., Hillaire-Marcel, C., & Kassou, N. (1992). Quantitative assessment of carbonate dissolution in marine sediments from foraminifers linings vs. shell ratios: Davis Strait, northwest North Atlantic. *Geology*, *20*(6), 527–530. https://doi.org/10.1130/0091-7613(1992)020%3C0527:QAOCDI%3E2.3.CO;2

de Vernal, A., Henry, M., Matthiessen, J., Mudie, P. J., Rochon, A., Boessenkool, K., … Voronina, E. (2001). Cyst assemblages as tracer of sea-surface conditions in the northern North Atlantic, Arctic and sub-Arctic seas: The "*n* = 677" database and derived transfer functions. *Journal of Quaternary Science*, *16*(7), 681–698. https://doi.org/10.1002/jqs.659

de Vernal, A., Rosell-Melé, A., Kucera, M., Hillaire-Marcel, C., Eynaud, F., Weinelt, M., … Kageyama, M. (2006). Comparing proxies for the reconstruction of LGM sea-surface conditions in the northern North Atlantic. *Quaternary Science Reviews*, *25*(21-22), 2820–2834. https://doi.org/10.1016/j.quascirev.2006.06.006

DeMaster, D. J. (1981). The supply and accumulation of silica in the marine environment. *Geochimica et Cosmochimica Acta*, *45*(10), 1715–1732. https://doi.org/10.1016/0016-7037(81)90006-5

Dickson, R., Rudels, B., Dye, S., Karcher, M., Meincke, J., & Yashayaev, I. (2007). Current estimates of freshwater flux through Arctic and subarctic seas. *Progress in Oceanography*, *73*(3-4), 210–230. https://doi.org/10.1016/j.pocean.2006.12.003

Dmitrenko, I. A., Kirillov, S. A., Rudels, B., Babb, D. G., Pedersen, L. T., Rysgaard, S., … Barber, D. G. (2017). Arctic Ocean outflow and glacier-ocean interaction modify water over the Wandel Sea shelf, northeast Greenland. *Ocean Science Discussions*, 1–47. https://doi.org/10.5194/os-2017-28

Fahl, K., & Stein, R. (2012). Modern seasonal variability and deglacial/Holocene change of central Arctic Ocean sea ice cover: New insights from biomarker proxy records. *Earth and Planetary Science Letters*, *351*(352), 123–133.

Fischer, G. (1991). Stable carbon isotope ratios of plankton carbon and sinking organic matter from the Atlantic sector of the Southern Ocean. *Marine Chemistry*, *35*(1-4), 581–596. https://doi.org/10.1016/S0304-4203(09)90044-5

Fripiat, F., Sigman, D. M., Fawcett, S. E., Rafter, P. A., Weigand, M. A., & Tison, J.-L. (2014). New insights into sea ice nitrogen biogeochemical dynamics from the nitrogen isotopes. *Global Biogeochemical Cycles*, *28*, 115–130. https://doi.org/10.1002/2013GB004729

Funder, S. (Ed.) 1989. Quaternary geology of the ice-free areas and adjacent shelves of Greenland. In R. J. Fulton (Ed.), *Quaternary geology of Canada and Greenland. The Geology of North America K-1* (pp. 741–792). Boulder, CO: Geological Society of America.

Funder, S., Kjeldsen, K. K., Kjær, K. H., Cofaigh, Ó., & C. (2011). The Greenland ice sheet during the past 300,000 years: A review. In J. Ehlers, P. L. Gibbard, & P. D. Hughes (Eds.), *Quaternary glaciations – extent and chronology – a closer look, Developments in Quaternary Sciences* (Vol. 15, pp. 699–714). Amsterdam: Elsevier. https://doi.org/10.1016/B978-0-444-53447-7.00050-7

Glud, R. N., Kühl, M., Wenzhöfer, F., & Rysgaard, S. (2002). Benthic diatoms of a High Arctic fjord (Young Sound, NE Greenland): importance for ecosystem primary production. *Marine Ecology Progress Series*, *238*, 15–29. https://doi.org/10.3354/meps238015

Glud, R. N., Woelfel, J., Karsten, U., Kühl, M., & Rysgaard, S. (2009). Benthic microalgal production in the Arctic: Applied methods and status of the current database. *Botanica Marina*, *52*, 559–571.

Goericke, R., & Fry, B. (1994). Variations of marine plankton delta-C-13 with latitude, temperature, and dissolved CO_2 in the world ocean. *Global Biogeochemical Cycles*, *8*(1), 85–90. https://doi.org/10.1029/93GB03272

Gradinger, R. (1995). Climate change and biological oceanography of the Arctic Ocean. *Philosophical Transactions: Physical Sciences and Engineering*, *352*(1699), 277–286. https://doi.org/10.1098/rsta.1995.0070

Hald, M., Dokken, T., Korsun, S., Polyak, L., & Aspeli, R. (1994). Recent and Late Quaternary distribution of *Elphidium excavatum* f. *clavata* in Arctic seas. *Cushman Foundation Special Publications*, *32*, 141–153.

Hald, M., & Korsun, S. (1997). Distribution of modern benthic foraminifera from fjords of Svalbard, European Arctic. *The Journal of Foraminifera Research*, *27*(2), 101–122. https://doi.org/10.2113/gsjfr.27.2.101

Hayes, J. M. (1993). Factors controlling ^{13}C contents of sedimentary organic compounds: Principles and evidence. *Marine Geology*, *113*(1-2), 111–125. https://doi.org/10.1016/0025-3227(93)90153-M

Heikkilä, M., Pospelova, V., Forest, A., Stern, G. A., Fortier, L., & Macdonald, R. W. (2016). Dinoflagellate cyst production over an annual cycle in seasonally ice-covered Hudson Bay. *Marine Micropaleontology*, *125*, 1–24. https://doi.org/10.1016/j.marmicro.2016.02.005

Heikkilä, M., Pospelova, V., Hochheim, K. P., Kuzyk, Z. Z. A., Stern, G. A., Barber, D. G., & Macdonald, R. W. (2014). Surface sediment dinoflagellate cysts from the Hudson Bay system and their relation to freshwater and nutrient cycling. *Marine Micropaleontology*, *106*, 79–109. https://doi.org/10.1016/j.marmicro.2013.12.002

Hemer, M. A., Post, A. L., O'Brien, P. E., Craven, M., Truswell, E. M., Roberts, D., & Harris, P. T. (2007). Sedimentological signatures of the sub-Amery Ice shelf circulation. *Antarctic Science*, *19*, 497–506.

Henriksen, N., Higgins, A. K., Kalsbeek, F., & Pulvertaft, T. C. R. (2000). Greenland from Archaean to Quaternary. Descriptive text to the Geological map of Greenland, 1:2 500 000. Geology of Greenland Survey Bulletin 185, 1–93 + map.

Henriksen, N., Higgins, A. K., Kalsbeek, F., & Pulvertaft, T. C. R. (2009). Greenland from Archaean to Quaternary. Descriptive text to the 1995 geological map of Greenland, 1:2 500 000. 2nd edition. Geological Survey of Denmark and Greenland Bulletin 18, 1–126 + map.

Higgins, A. K. (1991). North Greenland glacier velocities and calf ice production. *Polarforschung*, *60*(1), 1–23.

Hobson, K. A., Ambrose, W. G. Jr., & Renaud, P. E. (1995). Sources of primary production, benthic-pelagic coupling, and trophic relationships within the Northeast Water Polynya: Insights from $\delta^{13}C$ and $\delta^{15}N$ analysis. *Marine Ecology Progress Series*, *128*, 1–10. https://doi.org/10.3354/meps128001

Hobson, K. A., & Welch, H. E. (1992). Determination of trophic relationships within a High Arctic marine food web using $\delta^{13}C$ and $\delta^{15}N$ analysis. *Marine Ecology Progress Series*, *84*, 9–18. https://doi.org/10.3354/meps084009

Holland, M. M., Finnis, J., Barrett, A. P., & Serreze, M. C. (2007). Projected changes in Arctic Ocean freshwater budgets. *Journal of Geophysical Research*, *112*, G04S55. https://doi.org/10.1029/2006JG000354

Hörner, T., Stein, R., Fahl, K., & Birgel, D. (2016). Post-glacial variability of sea ice cover, river run-off and biological production in the western Laptev Sea (Arctic Ocean)—A high-resolution biomarker study. *Quaternary Science Reviews*, *143*, 133–149. https://doi.org/10.1016/j.quascirev.2016.04.011

Jennings, A. E., & Helgadottir, G. (1994). Foraminiferal assemblages from the fjords and shelf of eastern Greenland. *Journal of Foraminiferal Research*, *24*(2), 123–144. https://doi.org/10.2113/gsjfr.24.2.123

Jennings, A. E., Walton, M. E., Cofaigh, C. Ó., Kilfeather, A., Andrews, J. T., Ortiz, J. D., … Dowdeswell, J. A. (2014). Paleoenvironments during Younger Dryas-Early Holocene retreat of the Greenland Ice Sheet from outer Disko Trough, central west Greenland. *Journal of Quaternary Science*, *29*(1), 27–40. https://doi.org/10.1002/jqs.2652

Jennings, A. E., Weiner, N. J., Helgadottir, G., & Andrews, J. T. (2004). Modern foraminiferal faunas of the southwestern to Northern Iceland shelf: Oceanographic and environmental controls. *Journal of Foraminiferal Research*, *34*(3), 180–207. https://doi.org/10.2113/34.3.180

Jepsen, H. F., & Kalsbeek, F. (1998). Precambrian evolution of North and North-East Greenland: Crystalline basement and sedimentary basins. *Polarforschung 68*, 153–160 (printed 2000)

Johannessen, T., Jansen, E., Flatøy, A., & Ravelo, A. C. (1994). The relationship between surface water masses, oceanographic fronts and paleoclimatic proxies in surface sediments of the Greenland, Iceland Norwegian seas. In R. Zahn, et al. (Eds.), *Carbon cycling in the glacial*

ocean: Constraints on the ocean's role in global change, NATO ASI Ser., Ser. 1 (Vol. 17, pp. 61–85). New York: Springer. https://doi.org/10.1007/978-3-642-78737-9_4

Jones, E. P., Anderson, L. G., Jutterström, S., & Swift, J. H. (2008). Sources and distribution of fresh water in the East Greenland Current. *Progress in Oceanography*, *78*(1), 37–44. https://doi.org/10.1016/j.pocean.2007.06.003

Kahru, M., Brotas, V., Manzano-Sarabia, M., & Mitchell, B. G. (2011). Are phytoplankton blooms occurring earlier in the Arctic? *Global Change Biology*, *17*(4), 1733–1739. https://doi.org/10.1111/j.1365-2486.2010.02312.x

Karsten, U., Schlie, C., Woelfel, J., & Becker, B. (2011). Benthic diatoms in Arctic Seas—Ecological functions and adaptations. *Polarforschung*, *81*(2), 77–84.

Kelly, M. A., & Lowell, T. V. (2009). Fluctuations of local glaciers in Greenland during latest Pleistocene and Holocene time. *Quaternary Science Reviews*, *28*(21-22), 2088–2106. https://doi.org/10.1016/j.quascirev.2008.12.008

Kerby, N. W., & Raven, J. A. (1985). Transport and fixation of inorganic carbon by marine algae. *Advances in Botanical Research*, *11*, 71–123. https://doi.org/10.1016/S0065-2296(08)60169-X

Kirillov, S., Dmitrenko, I., Rysgaard, S., Babb, D., Pedersen, L. T., Ehn, J., … Barber, D. (2017). Storm-induced water dynamics and thermohaline structure of the tidewater Flade Isblink Glacier outlet to the Wandel Sea (NE Greenland). *Ocean Science*, *13*(6), 947–959. https://doi.org/10.5194/os-13-947-2017

Koç, N., Jansen, E., & Haflidason, H. (1993). Paleoceanographic reconstruction of surface ocean conditions in the Greenland, Iceland, and Norwegian seas through the last 14,000 years based on diatoms. *Quaternary Science Reviews*, *12*(2), 115–140. https://doi.org/10.1016/0277-3791(93)90012-B

Kohlbach, D., Graeve, M., Lange, A. B., David, C., Peeken, I., & Flores, H. (2016). The importance of ice algae-produced carbon in the central Arctic Ocean ecosystem: Food web relationships revealed by lipid and stable isotope analyses. *Limnology and Oceanography*, *61*(6), 2027–2044. https://doi.org/10.1002/lno.10351

Korsun, S., & Hald, M. (1998). Modern benthic foraminifera of Novaya Zemlya tidewater glaciers, Russian Arctic. *Arctic and Alpine Research*, *30*(1), 61–77. https://doi.org/10.2307/1551746

Korsun, S., & Hald, M. (2000). Seasonal dynamics of benthic foraminifera in a glacially fed fjord of Svalbard, European Arctic. *Journal of Foraminiferal Research*, *30*(4), 251–271. https://doi.org/10.2113/0300251

Kühl, M., Glud, R. N., Borum, R., Roberts, R., & Rysgaard, S. (2001). Photosynthetic performance of surface-associated algae below sea ice as measured with a pulse-amplitude-modulated (PAM) fluorometer and O_2 microsensors. *Marine Ecology Progress Series*, *223*, 1–14. https://doi.org/10.3354/meps223001

Kumar, V., Tiwari, M., Nagoji, S., & Tripathi, S. (2016). Evidence of Anomalously low d^{13}C of marine organic matter in an Arctic fjord. *Scientific Reports*, *6*(1), 36192. https://doi.org/10.1038/srep36192

Kunz-Pirrung, M. (1998). Aquatic palynomorphs: Reconstruction of Holocene sea-surface water masses in the eastern Laptev Sea. *Berichte zür Polarforschung*, *281*. ISSN 0176–5027

Kunz-Pirrung, M. (1999). Distribution of aquatic palynomorphs in surface sediments from the Laptev Sea, Eastern Arctic Ocean. In H. Kassens, et al. (Eds.), *Land-ocean systems in the Siberian Arctic: Dynamics and history* (pp. 561–575). Berlin: Springer. https://doi.org/10.1007/978-3-642-60134-7_43

Leslie, R. J. (1965). Ecology and paleoecology of Hudson Bay foraminifera. *Bedford Institute of Oceanography Report*, *65–6*, 192.

Linke, P., & Lutze, G. (1993). Microhabitat preferences of benthic foraminifera—A static concept or a dynamic adaptation to optimize food acquisition? *Marine Micropaleontology*, *20*(3-4), 215–234. https://doi.org/10.1016/0377-8398(93)90034-U

Loeng, H., Brander, K., Carmack, E., Denisenko, S., Drinkwater, K., Hanse, B., … Sakshaug, E. (2005). Marine systems. In C. Symon, L. Arris, & B. Heal (Eds.), *Arctic climate impact assessment* (pp. 453–538). New York: Cambridge University Press.

Lubinski, D. J., Polyak, L., & Forman, S. L. (2001). Freshwater and Atlantic water inflows to the deep northern Barents and Kara Seas since ca 13 ^{14}C ka: Foraminifera and stable isotopes. *Quaternary Science Reviews*, *20*(18), 1851–1879. https://doi.org/10.1016/S0277-3791(01)00016-6

Mackensen, A., & Hald, M. (1988). *Cassidulina teretis* Tappan and *C. laevigata* D'Orbigny: Their modern and Late Quaternary distribution in Northern Seas. *Journal of Foraminiral Research*, *18*(1), 16–24. https://doi.org/10.2113/gsjfr.18.1.16

MacIntyre, H. L., Geider, R. J., & Miller, D. C. (1996). Microphytobenthos: The ecological role of the "Secret Garden" of unvegetated, shallow-water marine habitats. I. Distribution, abundance and primary production. *Estuaries*, *19*(2), 186–201. https://doi.org/10.2307/1352224

Matthiessen, J., Baumann, K.-H., Schröder-Ritzrau, A., Hass, C., Andruleit, H., Baumann, A., … Thiede, J. (2001). Distribution of calcareous, siliceous and organic-walled planktic microfossils in surface sediments of the Nordic Seas and their relation to surface-water masses. In P. Schäfer, et al. (Eds.), *The Northern North Atlantic: A changing environment* (pp. 105–127). Berlin: Springer. https://doi.org/10.1007/978-3-642-56876-3_7

Matthiessen, J., Kunz-Pirrung, M., & Mudie, P. J. (2000). Freshwater chlorophycean algae in recent marine sediments of the Beaufort, Laptev and Kara Seas (Arctic Ocean) as indicators of river runoff. *International Journal of Earth Sciences*, *89*(3), 470–485. https://doi.org/10.1007/s005310000127

Mauritzen, C., & Hakkinen, S. (1997). Influence of sea ice on the thermohaline circulation in the Arctic-North Atlantic Ocean. *Geophysical Research Letters*, *24*(24), 3257–3260. https://doi.org/10.1029/97GL03192

Meire, L., Mortensen, J., Meire, P., Juul-Pedersen, T., Sejr, M. K., Rysgaard, S., … Meysman, F. J. R. (2017). Marine-terminating glaciers sustain high productivity in Greenland fjords. *Global Change Biology*, *23*(12), 5344–5357. https://doi.org/10.1111/gcb.13801

Meyers, P. A. (1994). Preservation of elemental and isotopic source identification of sedimentary organic matter. *Chemical Geology*, *114*(3-4), 289–302. https://doi.org/10.1016/0009-2541(94)90059-0

Meyers, P. A. (1997). Organic geochemical proxies of paleoceanographic, paleolimnologic, and paleoclimatic processes. *Organic Geochemistry*, *27*(5-6), 213–250. https://doi.org/10.1016/S0146-6380(97)00049-1

Milzer, G., Giraudeau, J., Faust, J., Knies, J., Eynaud, F., & Rühlemann, C. (2013). Spatial distribution of benthic foraminiferal stable isotopes and dinocyst assemblages in surface sediments of the Trondheimsfjord, central Norway. *Biogeosciences*, *10*(7), 4433–4448. https://doi.org/10.5194/bg-10-4433-2013

Montresor, M., Lovejoy, C., Orsini, L., Procaccini, G., & Roy, S. (2003). Bipolar distribution of the cyst-forming dinoflagellate *Polarella glacialis*. *Polar Biology*, *26*, 186–194.

Montresor, M., Procaccini, G., & Stoecker, D. K. (1999). *Polarella glacialis*, gen. Nov., sp. nov. (Dinophyceae): Suessiaceae are still alive! *Journal of Phycology*, *35*(1), 186–197. https://doi.org/10.1046/j.1529-8817.1999.3510186.x

Mudie, P. J., Keen, C. E., Hardy, I. A., & Vilks, G. (1983). Multivariate analysis and quantitative paleoecology of benthic foraminifera in surface and late Quaternary shelf sediments, northern Canada. *Marine Micropaleontology*, *8*, 283–313.

Mueller, D. R., Warwick, F. V., & Jeffries, M. O. (2003). Break-up of the largest Arctic ice shelf and associated loss of an epishelf lake. *Geophysical Research Letters 30*(20), 2031 https://doi.org/10.1029/2003GL017931

Müller, J., Masse, G., Stein, R., & Belt, S. T. (2009). Variability of sea ice conditions in the Fram Strait over the past 30,000 years. *Nature Geoscience*, *2*(11), 772–776. https://doi.org/10.1038/ngeo665

Mullin, J., & Riley, J. (1955). The colorimetric determination of silicate with special reference to sea and natural waters. *Analytica Chimica Acta*, *12*, 162–176. https://doi.org/10.1016/S0003-2670(00)87825-3

Naidu, A. S., Cooper, L. W., Finney, B. P., Macdonald, R. W., Alexander, C., & Semiletov, I. P. (2000). Organic carbon isotope ratios (d13C) of Arctic Amerasian continental shelf sediments. *International Journal of Earth Sciences*, *89*(3), 522–532. https://doi.org/10.1007/s005310000121

Niebauer, H. J., Alexander, V., & Henrichs, S. M. (1990). Physical and biological oceanographic interaction in the spring bloom at the Bering Sea marginal ice edge zone. *Journal of Geophysical Research*, *95*(C12), 22,229–22,241. https://doi.org/10.1029/JC095iC12p22229

Nørgaard-Pedersen, N., Mikkelsen, N., & Kristoffersen, Y. (2008). Late glacial and Holocene marine records from the Independence Fjord and Wandel Sea regions, North Greenland. *Polar Research*, *27*(2), 209–221. https://doi.org/10.1111/j.1751-8369.2008.00065.x

Nørgaard-Pedersen, N., Mikkelsen, N., Lassen, S. J., Kristoffersen, Y., & Sheldon, E. (2007). Reduced sea ice concentrations in the Arctic Ocean during the last interglacial period revealed by sediment cores off northern Greenland. *Paleoceanography*, *22*, PA1218. https://doi.org/10.1029/2006PA001283

Nørgaard-Pedersen, N., Ribeiro, S., Mikkelsen, N., Limoges, A., & Seidenkrantz, M.-S. (2016). Past climate and sea ice variability studies in the fjord area by Station Nord, eastern North Greenland. *Geological Survey of Denmark and Greenland Bulletin*, *35*, 67–70.

Nöthig, E.-M., Bracher, A., Engel, A., Metfies, K., Niehoff, B., Peeken, I., … Wurst, M. (2015). Summertime plankton ecology in Fram Strait—A compilation of long- and short-term observations. *Polar Research*, *34*(1), 23,349. https://doi.org/10.3402/polar.v34.23349

Pabi, S., van Dijken, G. L., & Arrigo, K. R. (2008). Primary production in the Arctic Ocean, 1998–2006. *Journal of Geophysical Research*, *113*(C8), C08005. https://doi.org/10.1029/2007JC004578

Pawlowski, J. (1991). Distribution and taxonomy of some benthic tiny foraminifers from the Bermuda Rise. *Micropaleontology*, *37*(2), 163–172. https://doi.org/10.2307/1485556

Perner, K., Moros, M., Lloyd, J. M., Jansen, E., & Stein, R. (2015). Mid to late Holocene strengthening of the East Greenland Current linked to warm subsurface Atlantic water. *Quaternary Science Reviews*, *129*, 296–307. https://doi.org/10.1016/j.quascirev.2015.10.007

Peterson, B. J., McClelland, J., Curry, R., Holmes, R. M., Walsh, J. E., & Aagaard, K. (2006). Trajectory shifts in the Arctic and Subarctic freshwater cycle. *Science*, *313*(5790), 1061–1066. https://doi.org/10.1126/science.1122593

Pineault, S., Tremblay, J.-E., Gosselin, M., Thomas, H., & Shadwick, E. (2013). The isotopic signature of particulate organic C and N in bottom ice: Key influencing factors and applications for tracing the fate of ice-algae in the Arctic Ocean. *Journal of Geophysical Research: Oceans*, *118*(1), 287–300. https://doi.org/10.1029/2012JC008331

Polyak, L., Alley, R. B., Andrews, J. T., Brigham-Grette, J., Cronin, T. M., Darby, D. A., … Wolff, E. (2010). History of sea ice in the Arctic. *Quaternary Science Reviews*, *29*(15-16), 1757–1778. https://doi.org/10.1016/j.quascirev.2010.02.010

Polyak, L., Korsun, S., Febo, L. A., Stanovoy, V., Khusid, T., Hald, M., … Lubinski, D. J. (2002). Benthic foraminiferal assemblages from the southern Kara Sea, a river-influenced Arctic marine environment. *Journal of Foraminiferal Research*, *32*(3), 252–273. https://doi.org/10.2113/32.3.252

Polyak, L., Levitan, M., Khusid, T., Merklin, L., & Mukhina, V. (2002). Variations in the influence of riverine discharge on the Kara Sea during the last deglaciation and the Holocene. *Global and Planetary Change*, *32*(4), 291–309. https://doi.org/10.1016/S0921-8181(02)00072-3

Polyak, L., & Mikhailov, V. (1996). Post-glacial environments of the southeastern Barents Sea: foraminiferal evidence. In J. T. Andrews, et al. (Eds.), *Late Quaternary palaeoceanography of the North Atlantic margins, Geological Society Special Publication* (Vol. 111, pp. 323–337).

Quaijtaal, W., Mertens, K. N., & Louwye, S. (2014). Some new acritarch species from the lower and middle Miocene of the Porcupine Basin, North Atlantic Ocean: biostratigraphy and palaeoecology. *Palynology*, *39*(1), 37–55.

Rau, G. H., Takahashi, T., Desmarais, D. J., Repeta, D. J., & Martin, J. H. (1992). The relationship between $\delta^{13}C$ or organic matter and CO_2 [aq] in ocean surface-water—Data from a JGOFS site in the northeast Atlantic Ocean and a model. *Geochimica et Cosmochimica Acta*, *56*(3), 1413–1419. https://doi.org/10.1016/0016-7037(92)90073-R

Rau, G. H., Takahashi, T., & Marias, D. J. (1989). Latitudinal variations in plankton $\delta^{13}C$: implications for CO_2 and productivity in the past oceans. *Nature*, *341*(6242), 516–518. https://doi.org/10.1038/341516a0

Ribeiro, S., Sejr, M. K., Limoges, A., Heikkilä, M., Andersen, T. J., Tallberg, P., … Rysgaard, S. (2017). Sea ice and primary production proxies in surface sediments from a High Arctic Greenland fjord: Spatial distribution and implications for palaeoenvironmental studies. *Ambio*, *46*(S1), 106–118. https://doi.org/10.1007/s13280-016-0894-2

Robinson, R. S., Kienast, M., Albuquerque, A. L., Altabet, M., Contreras, S., De Pol Holz, R., … Yang, J.-Y. (2012). A review of nitrogen isotopic alteration in marine sediments. *Paleoceanography*, *27*, PA4203. https://doi.org/10.1029/2012PA002321

Rochon, A., de Vernal, A., Turon, J. L., Matthiessen, J., & Head, M. J. (1999). *Distribution of. dinoflagellate cysts in surface sediments from the North Atlantic Ocean and adjacent basin and quantitative reconstruction of sea-surface parameters, Contribution Series* (Vol. 35, p. 152). Dallas: American Association of Stratigraphic Palynologists.

Rysgaard, S., Vang, T., Stjernholm, M., Rasmussen, B., Windelin, A., & Kiilsholm, S. (2003). Physcial conditions, carbon transport and climate change impacts in a NE Greenland fjord. *Arctic, Antarctic, and Alpine Research*, *35*(3), 301–312. https://doi.org/10.1657/1523-0430(2003)035%5B0301:PCCTAC%5D2.0.CO;2

Salvi, C., Busetti, M., Marinoni, L., & Brambati, A. (2006). Late Quaternary glacial marine to marine sedimentation in the Pennell Trough (Ross Sea, Antarctica). *Paleogeography, Palaeoclimatology, Palaeoecology*, *231*(1-2), 199–214. https://doi.org/10.1016/j.palaeo.2005.07.034

Schroeder-Adams, C., & van Rooyen, D. (2011). Response of recent benthic foraminiferal assemblages to contrasting environments in Baffin Bay and the Northern Labrador Sea, Northwest Atlantic. *Arctic*, *64*(3), 317–341.

Schubert, C. J., & Calvert, S. E. (2001). Nitrogen and carbon isotopic composition of marine and terrestrial organic matter in Arctic Ocean sediments: Implications for nutrient utilization and organic matter composition. *Deep-Sea Research Part I*, *48*(3), 789–810. https://doi.org/10.1016/S0967-0637(00)00069-8

Seidenkrantz, M.-S. (1995). *Cassidulina teretis* Tappan and *Cassidulina neoteretis* new species (Foraminifera): stratigraphic markers for deep sea and outer shelf areas. *Journal of Micropalaeontology*, *14*(2), 145–157. https://doi.org/10.1144/jm.14.2.145

Seidenkrantz, M.-S., Aagaard-Sørensen, S., Møller, H. S., Kuijpers, A., Jensen, K. G., & Kunzendorf, H. (2007). Hydrography and climatic change during the last 4.400 years in Ameralik Fjord, SW Greenland. *The Holocene*, *17*(3), 387–401. https://doi.org/10.1177/0959683607075840

Seidenkrantz, M.-S., Ebbesen, H., Aagaard-Sørensen, S., Moros, M., Lloyd, J., Olsen, J., … Kuijpers, A. (2013). Early Holocene large-scale meltwater discharge from Greenland documented by foraminifera and sediment parameters. *Paleogeography, Palaeoclimatology, Palaeoecology*, *391*, 71–81. https://doi.org/10.1016/j.palaeo.2012.04.006

Sejr, M. K., Stedmon, C. A., Bendtsen, J., Abermann, J., Pedersen, T. J., Mortsensen, J., & Rysgaard, S. (2017). Evidence of local and regional freshening of East Greenland coastal waters. *Scientific Reports*, *7*(1), 1318313183. https://doi.org/10.1038/s41598-017-10610-9

Smetacek, V., & Nicol, S. (2005). Polar ocean ecosystems in a changing world. *Nature*, *437*(7057), 362–368. https://doi.org/10.1038/nature04161

Smik, L., Cabedo-Sanz, P., & Belt, S. T. (2016). Semi-quantitative estimates of paleo Arctic sea ice concentration based on source-specific highly branched isoprenoid alkenes: A further development of the PIP25 index. *Organic Geochemistry*, *92*, 63–69. https://doi.org/10.1016/j.orggeochem.2015.12.007

Søreide, J. E., Hop, H., Carroll, M. L., Falk-Petersen, S., & Hegseth, N. E. (2006). Seasonal food web structures and sympagic–pelagic coupling in the European Arctic revealed by stable isotopes and a two-source food web model. *Progress in Oceanography*, *71*(1), 59–87. https://doi.org/10.1016/j.pocean.2006.06.001

Sorrel, P., Popescu, S.-M., Head, M. J., Suc, J. P., Klotz, S., & Oberhänsli, H. (2006). Hydrographic development of the Aral Sea during the last 2000 years based on a quantitative analysis of dinoflagellate cysts. *Paleogeography, Palaeoclimatology, Palaeocology*, *234*(2-4), 304–327. https://doi.org/10.1016/j.palaeo.2005.10.012

Stabeno, P. J., Napp, J., Mordy, C., & Whitledge, T. (2010). Factors influencing physical structure and lower trophic levels of the eastern Bering Sea shelf in 2005: Sea ice, tides, and winds. *Progress in Oceanography*, *85*(3-4), 180–196. https://doi.org/10.1016/j.pocean.2010.02.010

Stein, R., Fahl, K., & Müller, J. (2012). Proxy reconstruction of Cenozoic Arctic Ocean sea ice history—From IRD to IP_{25}. *Polarforschung*, *82*, 37–71.

Stein, R., Grobe, H., & Wahsner, M. (1994). Organic carbon, carbonate, and clay mineral distributions in eastern central Arctic Ocean surface sediments. *Marine Geology*, *119*(3-4), 269–285. https://doi.org/10.1016/0025-3227(94)90185-6

Steinsund, P. I., Polyak, L., Hald, M., Mikhailov, V., & Korsun, S. (1994). Distribution of calcareous benthic foraminifera in recent sediments of the Barents and Kara Seas. In: Steinsund, P.I., *Benthic foraminifera in surface sediments of the Barents and Kara Seas: Modern and late Quaternary application* (PhD thesis). (pp. 61–102). Department of Geology, Institute of Biology and Geology, University of Tromsø, Norway.

Stockmarr, J. (1971). Tablets with spores used in absolute pollen analysis. *Pollen et Spores*, *13*, 615–621.

Stoecker, D. K., Gustafson, D. E., Merrell, J. R., Black, M. M. D., & Baier, C. T. (1997). Excystment and growth of chrysophytes and dinoflagellates at low temperatures and high salinities in Antarctic sea-ice. *Journal of Phycology*, *33*(4), 585–595. https://doi.org/10.1111/j.0022-3646.1997.00585.x

Sutherland, D. A., & Pickart, R. S. (2008). The East Greenland Coastal Current: Structure, variability, and forcing. *Progress in Oceanography*, *78*(1), 58–77. https://doi.org/10.1016/j.pocean.2007.09.006

Tremblay, G., Belzile, C., Gosselin, M., Poulin, M., Roy, S., & Tremblay, J. E. (2009). Late summer phytoplankton distribution along a 3500 km transect in Canadian Arctic waters: Strong numerical dominance by picoeukaryotes. *Aquatic Microbial Ecology*, *54*, 55–70. https://doi.org/10.3354/ame01257

Tremblay, J.-E., Anderson, L. G., Matrai, P., Coupel, P., Bélanger, S., Michel, C., & Reigstad, M. (2015). Global and regional drivers of nutrient supply, primary production and CO_2 drawdown in the changing Arctic Ocean. *Progress in Oceanography*, *139*, 171–196. https://doi.org/10.1016/j.pocean.2015.08.009

Vare, L. L., Massé, G., & Belt, S. T. (2010). A biomarker-based reconstruction of sea ice conditions for the Barents Sea in recent centuries. *Holocene*, *20*(4), 637–643. https://doi.org/10.1177/0959683609355179

Vare, L. L., Massé, G., Gregory, T. R., Smart, C. W., & Belt, S. T. (2009). Sea ice variations in the central Canadian Arctic Archipelago during the Holocene. *Quaternary Science Reviews*, *28*(13-14), 1354–1366. https://doi.org/10.1016/j.quascirev.2009.01.013

Volkmann, R. (2000). Planktic foraminifers in the outer Laptev Sea and the Fram Strait—Modern distribution and ecology. *Journal of Foraminiferal Research*, *30*(3), 157–176. https://doi.org/10.2113/0300157

Wollenburg, J. E., & Kuhnt, W. (2000). The response of benthic foraminifers to carbon flux and primary production in the Arctic Ocean. *Marine Micropaleontology*, *40*(3), 189–231. https://doi.org/10.1016/S0377-8398(00)00039-6

Wollenburg, J. E., & Mackensen, A. (1998). Living benthic foraminifera from the central Arctic Ocean: Faunal composition, standing stock and diversity. *Marine Micropaleontology*, *34*(3-4), 153–185. https://doi.org/10.1016/S0377-8398(98)00007-3

Wulff, A., Iken, K., Quartino, M. L., Al-Handal, A., Wiencke, C., & Clayton, M. N. (2009). Biodiversity, biogeography and zonation of benthic micro- and macroalgae in the Arctic and Antarctic. *Botanica Marina*, *52*, 491–507.

Wulff, A., Roleda, M. Y., Zacher, K., & Wiencke, C. (2008). Exposure to sudden light burst after prolonged darkness—A case study on benthic diatoms in Antarctica. *Diatom Research*, *23*(2), 519–532. https://doi.org/10.1080/0269249X.2008.9705774

Xiao, X., Fahl, K., & Stein, R. (2013). Biomarker distribution in surface sediments from the Kara and Laptev seas (Arctic Ocean): Indicators for organic-carbon sources and sea-ice coverage. *Quaternary Science Reviews*, *79*, 40–52. https://doi.org/10.1016/j.quascirev.2012.11.028

Zamelczyk, K., Rasmussen, T. L., Husum, K., Haflidason, H., de Vernal, A., Ravna, E. K., … Hillaire-Marcel, C. (2012). Paleoceanographic changes and calcium carbonate dissolution in the central Fram Strait during the last 20 ka yr. *Quaternary Research*, *78*(03), 405–416. https://doi.org/10.1016/j.yqres.2012.07.006

Zheng, S., Wang, G., & Lin, S. (2012). Heat shock effects and population survival in the polar dinoflagellate *Polarella glacialis*. *Journal of Experimental Marine Biology and Ecology*, *438*, 100–108. https://doi.org/10.1016/j.jembe.2012.09.003

Zonneveld, K. A. F., Versteegh, G. J. M., & Kodrans-Nsiah, M. (2008). Preservation and organic chemistry of Late Cenozoic organic-walled dinoflagellate cysts: A review. *Marine Micropaleontology*, *68*(1-2), 179–197. https://doi.org/10.1016/j.marmicro.2008.01.015